UNIVERSITY OF CALIFORNIA
RIVERSIDE

Osmoregulatory Impacts of Triphenyl Phosphate on Zebrafish Embryos

A Dissertation submitted in partial satisfaction
of the requirements for the degree of

Doctor of Philosophy

in

Environmental Sciences

by

Jenna Wiegand

June 2023

Dissertation Committee:
Dr. David Volz, Chairperson
Dr. Daniel Schlenk
Dr. Jay Gan

The Dissertation of Jenna Wiegand is approved:

_____

_____

_____

Committee Chairperson

University of California, Riverside

Acknowledgements

This dissertation has been completed with the help and support of many individuals. First, I would like to thank my advisor, Dr. David Volz, for continuing to motivate, mentor, and support me through these past four years, and through a pandemic. He has helped me come into my own as a scientist, as well as working to continually adapt methods, ideas, and our laboratory space to ensure my accessibility needs were met. His commitment towards making me a better researcher is one of the main reasons I was able to complete this dissertation. I would also like to thank the following members who have served on my committees over the past four years for the advice and guidance: Dr. Daniel Schlenk, Dr. Jay Gan, Dr. Andrew Gray, and Dr. Changcheng Zhou.

I would also like to thank the past and present members of my lab. I would like to thank Dr. Aalekya Reddam, Dr. Vanessa Cheng, Sarah Avila-Barnard, and John Hoang, for making the West Coast feel like home and always being there to brainstorm when things went wrong and celebrate whenever something went right. I can't thank you enough for being wonderful friends and bringing so much love, laughter, and adventure into my time at UCR.

This research was support by UCR's Graduate Division, the NRSA T32 Training Program (T32ES018827), a National Institute of Health grant (R01ES027576), and a USDA National Institute of Food and Agriculture Hatch Project (1009609).

Copyright Acknowledgements

The text and figures in Chapter 2, in part or in full, are a reprint of the material as it appears in “Triphenyl phosphate-induced pericardial edema is associated with elevated epidermal ionocytes within zebrafish embryos” published in Environmental Toxicology and Pharmacology, Vol 89, 2022. The co-authors Vanessa Cheng, Aalekya Reddam, and Sarah Avila-Barnard helped in methodology and investigation. The co-author David C. Volz directed and supervised this research.

The text and figures in Chapter 3, in part or in full, are a reprint of the materials as it appears in “Triphenyl phosphate-induced pericardial edema in zebrafish embryos is dependent on the ionic strength of exposure media” published in Environment International, Vol 173, 2023. The co-authors Sarah Avila-Barnard, Charvita Nemarugommula, David Lyons, and Sharon Zhang helped in methodology and investigation. The co-author Heather M. Stapleton helped with resources, writing review and editing, as well as project supervision and administration. The co-author David C. Volz directed and supervised this research.

All supplementary materials reported in this dissertation are available through ProQuest Dissertation & Theses.

Dedication

To everyone who has supported me through this process. To Philip Sumberaz for standing by my side for the last eight years. To Sarah Avila- Barnard for motivating me to be my best self, while still taking care of myself. To Matthew LeFauve for being a wonderful mentor. Finally, to my family for cheering me on from the sidelines and believing in me. I couldn't have done this without you all!

ABSTRACT OF THE DISSERTATION

Osmoregulatory Impacts of Triphenyl Phosphate on Zebrafish Embryos

by

Jenna Wiegand

Doctor of Philosophy, Graduate Program in Environmental Sciences
University of California, Riverside, June 2023
Dr. David Volz, Chairperson

Triphenyl phosphate (TPHP) is an organophosphate ester-based plasticizer and flame retardant that is used worldwide and detected at elevated levels within environmental media such as surface water, dust, and sediments. Past studies have found that TPHP causes adverse phenotypes within embryonic zebrafish when exposed from 24-72 h post fertilization (hpf), including prevention of cardiac looping due to pericardial edema. TPHP is not the only environmental contaminant that is known to cause pericardial edema in embryonic zebrafish, as over 35 other chemicals have been found to cause pericardial edema. However, little is known about the mechanism leading to edema formation within fish embryos even though there are numerous studies that have investigated the mechanisms underlying edema within mammalian models and humans. In Chapter 2, we will determine whether TPHP exposure disrupts the abundance of Na+/K+ ionocytes in early embryonic development within zebrafish. In Chapter 3, we will determine whether media ionic strength affects the toxicity of TPHP within embryonic zebrafish, including potential impacts on the yolk sac epithelium. In Chapter 4, we will determine how TPHP induces injury to the yolk sac epithelium by focusing on potential effects on prolactin abundance and wound repair, as well as whether TPHP-induced

pericardial edema is reversible or irreversible. Overall, using TPHP as a reference chemical, we expect our findings will increase our understanding of mechanisms underlying chemically-induced edema formation within embryonic zebrafish.

Table of Contents

List of Figures

Chapter 2

Chapter 3

Chapter 4

Chapter 5

Chapter 1: Introduction and Literature Review

Section 1.1: Role of Osmoregulation in Fish Physiology

Similar to many other vertebrate species, fish maintain ionic and osmotic homeostasis to ensure optimal cellular and physiological processes (Guh et al., 2015). This process is achieved by utilizing transepithelial transport mechanisms, very similar to what is observed in humans (Guh et al., 2015). However, there is a major difference between fish vs. humans, as fish need to balance ionic and osmotic gradients between their outward aquatic environment and internal system (Guh et al., 2015). This process has evolved to be accurate and adapt quickly to changes in the environment, which can vary in osmolarity and ionic composition (Guh et al., 2015). Fish perform many of their ionic and osmoregulatory mechanisms in their gills, which take on a similar role as the human kidney (Evans, 2008; Hwang & Lee, 2007). Within the gills, ionocytes represent major, mitochondria-rich cells that are responsible for the transport of ions (mainly Na^+, Cl^-, Ca^{2+}, H^+, HCO^3-, and NH^4 in freshwater fish) and are functionally analogous to mammalian renal tubular cells (Dymowska et al., 2012; Evans, 2011; Guh et al., 2015; Hwang et al., 2011).

After fertilization of zebrafish eggs, ionocytes begin to differentiate at approximately 24 h post-fertilization (hpf) and are localized along the embryonic skin in order to allow transport of essential ions from the surrounding water into the developing embryo (Hwang & Chou, 2013). During maturation, ionocytes migrate to the developing gills and the number of epidermal ionocytes decrease. After all ionocytes have migrated to the gills, the number of ionocytes ceases to increase (Ayson et al., 1994; Hiroi et al., 1999). Within adults, localization of ionocytes within the gills provides adequate respiratory and osmoregulatory capacity in order to meet the physiological demands of the organism (Rombough, 2007).

Zebrafish has been extensively used as a model to investigate mechanisms underlying osmoregulation in freshwater fish (Evans, 2011; Guh et al., 2015; Kumai & Perry, 2012; Kwong et al., 2013; Kwong & Perry, 2013). Within zebrafish, five types of ionocytes have been identified: (1) H^+ ATPase rich (HR), (2) Na^+K^+ ATPase-rich (NaR), (3) Na^+Cl^- cotransporter expressing (NCC), (4) solute carrier family 26 (SLC26)-expressing, and (5) K^+ secreting (KS) ionocytes; each of these cells have different sets of ion transporters responsible for (1) H^+ secretion/Na^+ uptake/$NH4^+$ excretion, (2) Ca^{2+} uptake, (3) Na^+/Cl^- uptake, K^+ secretion, (4) Cl^- uptake/HCO^{3-} secretion, and (5) excretion of ions, respectively (Hwang et al., 2011; Hwang & Chou, 2013). Freshwater ionocytes have apical surfaces that form microvilli (Hwang, 1988; Marshall et al., 1997; Stainier & Fishman, 1992). Importantly, freshwater fish do not always have the same ionocyte structure, as there are a few exceptions to the general structure above. The mechanisms underlying ion transport in freshwater fish are more complicated than in saltwater fish. There are more ionocyte types and subtypes observed in freshwater species, and these ionocytes vary depending on the fish's native environment (Breves et al., 2020; Dymowska et al., 2012; Hiroi & McCormick, 2012; Hsu et al., 2014; Hwang et al., 2011). These species-specific differences reflect the evolution of different ion uptake mechanisms (Hwang & Chou, 2013) due to changing freshwater environments with a wide range of ion compositions (Dymowska et al., 2012; Fridman, 2020; Takei et al., 2014; Yan & Hwang, 2019).

Ionocytes are derived from non-neural ectoderm that express ΔNp63 – a transcription factor required for the proliferation of epithelial cells (Carney et al., 2007). After gastrulation, two specification markers for ionocytes are expressed in specific ΔNp63-positive epidermal cells – forkhead box I3a (Foxi3a) and Delta C, which is a ligand for Notch signaling. These cells then differentiate into ionocyte progenitors (Carney et al.,

2007; Hsiao et al., 2007), and Notch signaling maintains cell fate after ionocyte progenitors progress through lateral inhibition by inhibiting Foxi3a expression. At the 14-somite stage, ΔNp63 expression in epidermal ionocyte progenitors is downregulated so Foxi3a can activate the differentiation of ionocytes (Carney et al., 2007; Hsiao et al., 2007). Although prior studies have established that Foxi3a plays a large role in ionocyte differentiation in zebrafish, little is known about the localization of epidermal ionocytes within embryos.

Homeostasis is achieved through active transporters. The regulation of ionocytes is important for the acclimation process of fish and tightly controlled by hormones (Evans, 2008; Takei et al., 2014). Prior studies have found that acclimation induces a change in ionocyte number in trout, eel, and guppy fish. This occurs during the acclimation process when salinity changes, which is thought to be caused by the turnover rate of cells and enhanced mitotic activity (Chretien & Pisam, 1986; Conte & Lin, 1967). Other studies have found that the expression and function of transporters are modified without corresponding changes in cell turnover when salinity levels are lower than normal over a period of a few days (Choi et al., 2011; Hiroi et al., 1999; Inokuchi & Kaneko, 2012; Lin et al., 2004). The changing number of ionocytes during environmental flux can also be based on the transformation of existing ionocytes. Reliance on one or both processes is dependent on the species of fish as well as the intensity of the environmental stressors (Guh et al., 2015).

In adult fish, ionocytes are found in the gill region, intestines, and kidneys. In freshwater fish, ionocytes are regulated by prolactin and cortisol (Chang & Hwang, 2011; Hwang & Chou, 2013). The presence of glucocorticoid receptor (GR) mRNA within multiple ionocytes in zebrafish gills (Lin et al., 2016) suggests that cortisol may play a direct role in ionic activity (Guh et al., 2015). For example, the proliferation and

differentiation of ionocytes in saltwater fish have been found to be regulated by cortisol, growth hormone (GH), and insulin-like growth factor 1 (IGF-I) (Chang & Hwang, 2011; Hwang & Chou, 2013).

To date, three types of ionocytes have been found in saltwater fish and five types of ionocytes have been found in freshwater fish – all of which are specialized for each living environment (Inokuchi et al., 2017; Leguen et al., 2015). In freshwater fish, the aquaphilic ionocytes regulate the uptake of ions through aquaporins which controls bodily fluids of the fish. In saltwater fish, halophilic ionocytes that transport ions out of the cell also control cell shrinkage by ensuring there is enough water uptake, a process that also utilizes aquaporins (Conte, 2012). In saltwater fish, general morphological characteristics have been determined. These traits include the apical membrane being recessed below the surface of the surrounding cells, forming what has been coined a “crypt” (Karnaky, 1986). The “crypt” can be shared with accessory cells (ACs), which are undifferentiated ionocytes localized adjacent to mature ionocytes (Hootman & Philpott, 1980). These cells create a “multi-cellular complex” with a cytoplasmic process of ACs, which can spread to the apical cytoplasm (Laurent, 1984; Wilson & Laurent, 2002). The current model for NaCl transport through ionocytes in saltwater teleosts includes three ion-transporting proteins: $Na^+/K^+/2Cl^-$ co-transporter, Na^+/K^+- ATPase (NKA), (NKCC1) and a Cl^- channel homologous to the human cystic fibrosis transmembrane receptor (CFTR) (Evans et al., 1999, 2005; Hirose et al., 2003; Hwang & Lin, 2013).

Aquaporins are found in most cells to allow water and ion flow into and out of the cell, and there are numerous forms of aquaporins to accommodate different cells around the body. Aquaporins have been found in a wide range of organisms including fish, mammals, and plants. In the case of ionocytes, aquaporins play a large role in osmoregulation (Kwong et al., 2013). Within zebrafish, there are currently four major

subfamilies identified – orthodox aquaporins (AQP1 and AQP4), aquaglyceroporins that transport glycerol and water (AQP3 and AQP7-10), water and urea transporter (AQP8), and unorthodox aquaporins (AQP11 and AQP12) (Tingaud-Sequeira et al., 2010). Past studies have found that AQP1 could potentially play a role in water absorption and osmoregulation, and zebrafish have two of these AQP1 homologues (Chen et al., 2010).

Section 1.2: Edema Formation in Embryos

Edema is an abnormal accumulation of fluid in the interstitium of the body's cavities and beneath the epidermal layer (Dejana et al., 2009). Edema can be caused by diseases or underlying illness as well as external factors that are causing damage to an organism. Edema is seen in most living organisms that retain fluid. The mechanisms underlying edema have been extensively studied within mammalian models and humans but, within the published literature specific to fish, edema is often described as a negative phenotype/endpoint in the absence of mechanistic investigations. Two of the most documented edema phenotypes are pericardial edema and yolk sac edema due to the ability and ease that both endpoints can be analyzed in a laboratory setting (Narumanchi et al., 2021). Despite the ease of analysis and widespread use of these endpoints, pericardial edema and yolk sac edema are often considered non-specific phenotypes due to the lack of knowledge about underlying mechanisms causing edema formation (Narumanchi et al., 2021).

Despite the lack of knowledge about the underlying mechanism that causes pericardial and yolk sac edema within fish embryos, previous studies have found factors which can lead to edema formation in embryonic zebrafish. These factors include pathogen exposure (Pikula et al., 2021), decreased number of tight junctions in embryonic fish skin (Kiener et al., 2008), increased permeability of fish skin (Kiener et al., 2008), high cortisol levels caused by injury and stress (Nesan & Vijayan, 2012), removal of ionocyte

transcription factors (Hsiao et al., 2007), reduced retinoic acid signaling (Begemann et al., 2004), intestinal damage and reduced mucus secretion (Thakur et al., 2014), infiltration of macrophages and neutrophils into injuries and globlet cell apoptosis (Xie et al., 2021), and upregulation of inflammatory genes (Thakur et al., 2014).

Section 1.3: Chemically-Induced Edema

One of the largest fields that utilizes pericardial edema and yolk sac edema as endpoints within fish embryos is toxicology. One paper compiled all of the studies that utilized zebrafish as a model for toxicology and listed all chemicals that caused negative phenotypes, including pericardial edema and yolk sac edema, up to 2011 (Mccollum et al., 2011). At the time of publication, 22 chemicals caused yolk sac edema and 35 chemicals caused pericardial edema to form in the embryos, making these the most observed phenotypes in the review (Mccollum et al., 2011). Since then, individual studies have found a multitude of chemicals which cause pericardial edema and/or yolk sac edema to form, including numerous studies from our lab. For example, we have found that exposure of embryonic zebrafish to triphenyl phosphate (TPHP) results in the formation of pericardial edema, a phenotype that has been reproducible across many studies since 2013 (Isales et al., 2015; McGee et al., 2013; Mitchell et al., 2018, 2019; Reddam et al., 2019).

One of the most studied contaminants that induces severe pericardial edema and yolk sac edema is 2,3,7,8-tetrachlorodibenzo-p-dioxin (TCDD). Although few of the studies focused on identifying the mechanism of action causing the edema, one study hypothesized that TCDD may be inhibiting the embryo's ability to create a permeability barrier to water which can impact the embryo's ability to maintain osmotic balance (Hill et al., 2004). Another hypothesis is that edema may be associated with leaks in the endothelial vessels, which often results in cardiovascular abnormalities (Oliveira et al.,

2009). Recent studies have found that an aryl hydrocarbon receptor 2 (ahr2) mutant is resistant to severe pericardial edema due to TCDD exposure, but little is known as to why this is occurring (Garcia et al., 2018; Goodale et al., 2012). Although mannitol blocks pericardial edema from forming in embryos when exposed to TPHP (Mitchell et al., 2019; Wiegand et al., 2022), mannitol was unable to fully reverse edema in TCDD-exposed embryos (Hill et al., 2004), indicating that 1) pericardial edema is likely caused by multiple mechanisms of action or 2) the concentration of mannitol was not high enough to counteract the severe impacts of TCDD.

Another well studied contaminant that induces pericardial edema is ethanol. It has been found to cause severe damage in embryonic zebrafish at a 2% concentration, which cannot be reversed or alleviated (Li et al., 2016; Pinheiro-da-Silva & Luchiari, 2021). It is believed that edema was caused by damaged blood vessels found in the embryo, resulting in a change in skin permeability and a decrease in the volume of blood (Li et al., 2016). Another hypothesis is that ethanol impacts the organization of the endothelial cell junctions in embryos (Dejana et al., 2009). Despite the number of contaminants causing pericardial and yolk sac edema, little is known about the mechanisms underlying edema formation in embryonic fish.

Section 1.4: Overview of Research Aims

While TPHP's impact on embryonic zebrafish has been previously studied within our lab, there are still knowledge gaps about why pericardial edema is forming during early development, and what TPHP is targeting in the embryo to cause its formation. To address knowledge gaps in how pericardial edema is being formed during TPHP exposure in early development, Chapter 2 will determine whether important aspects of the zebrafish embryo's osmoregulation system is being impacted by TPHP by relying on immunohistochemistry, co-exposures with D-mannitol and ouabain, morpholino

injections, and mRNA sequencing. Within Chapter 3, we will perform TPHP exposures and stain zebrafish embryos with a fluorescent sodium indicator dye to quantify embryonic sodium concentrations *in situ*, create different exposure media of varying ionic strength, quantify embryonic doses of TPHP and DPHP, a common metabolite of TPHP, characterize the ion content of various exposure media using ion chromatography and ICP-OES, and utilize a scanning electron microscope to analyze the skin of the embryonic zebrafish's yolk sac. In Chapter 4, we will utilize fenretinide and TPHP co-exposures to determine if fenretinide and D-mannitol block edema through different mechanisms, as well as investigate important aspects of the embryonic zebrafish epidermal layer to determine if TPHP is directly targeting the embryonic skin. We will also conduct recovery experiments to determine if edema caused by TPHP is a reversible or irreversible defect.

Chapter 2: Triphenyl Phosphate-Induced Pericardial Edema is Associated With Elevated Epidermal Ionocytes Within Zebrafish Embryos

2.1 Abstract

Triphenyl phosphate (TPHP) is an organophosphate ester-based plasticizer and flame retardant that is used worldwide and detected at elevated levels within environmental media such as surface water. The objective of this study was to identify the potential role of epidermal ionocytes in mediating TPHP-induced pericardial edema formation within zebrafish embryos. In addition to increased pericardial edema and decreased body length, exposure to TPHP from 24 to 72 h post fertilization (hpf) resulted in a significant increase in the number of ionocytes at 72 hpf relative to time-matched embryos treated with vehicle (0.1% DMSO). We also found that co-exposure of embryos to mannitol (an osmotic diuretic) from 24-72 hpf blocked TPHP-induced pericardial edema as well as effects on ionocyte abundance, suggesting that increased ionocytes were strongly associated with TPHP-induced edema formation. However, initiation of exposure at 30 hpf (vs. 24 hpf) mitigated TPHP-induced effects on ionocyte abundance at 72 hpf even though the magnitude of TPHP-induced pericardial edema and body length was similar following exposure from 24-72 hpf and 30-72 hpf, suggesting that 1) 24-30 hpf represents a critical window of exposure for TPHP induced effects on ionocyte abundance and 2) an increase in ionocyte abundance may not be required for pericardial edema formation. Interestingly, we found that knockdown of ATPase1a1.4 – an abundant Na^+/K^+-ATPase localized to epidermal ionocytes in zebrafish embryos – mitigated TPHP-induced effects on ionocyte abundance (but not pericardial area), whereas co-exposure of embryos to ouabain – a broad-spectrum Na^+/K^+-ATPase inhibitor – from 24-72 hpf enhanced TPHP induced effects on pericardial area (but not ionocyte abundance). Overall, our findings suggest that TPHP may have multiple mechanisms of toxicity leading

to an increase in ionocyte abundance and pericardial edema within developing zebrafish embryos.

2.2 Introduction

Triphenyl phosphate (TPHP) is an organophosphate ester (OPE) that is used worldwide as a plasticizer and additive flame retardant (van der Veen & de Boer, 2012). As a semi-volatile organic compound, TPHP is not chemically bound to polymers within end-use products and has the potential to readily migrate into the environment (Song et al., 2019), resulting in contamination of indoor dust (Dasgupta et al., 2021; Klose et al., 2021; Stapleton et al., 2009) sediment (Fan et al., 2021; Reemtsma et al., 2008), and surface water (Chen et al., 2021; Li et al., 2018; Reemtsma et al., 2008). The primary source of TPHP in the aquatic environment is wastewater discharge (Green et al., 2007; Kim et al., 2011), where TPHP concentrations can reach 66.7 µg/kg within sludge effluent samples collected from wastewater treatment plants (Gao et al., 2016) and up to 8,400 pg/L within samples collected from receiving surface waters (Li et al., 2017). Although TPHP is less persistent relative to other industrial chemicals such as brominated flame retardants (Kim et al., 2011; Yang et al., 2019), TPHP has the potential to bioaccumulate within aquatic organisms (Yang et al., 2019) and has been detected in fish muscle tissue up to 230 ng/g lipid weight (Matsukami et al., 2016) since TPHP use is ubiquitous and exposure is continuous (Liu et al., 2020; Ramesh et al., 2020; Yang et al., 2019).

As an industrial chemical with varying modes of action and mechanisms of toxicity, TPHP exposure of aquatic vertebrates leads to a wide range of adverse outcomes depending on the species, developmental stage, life history, etc. For example, TPHP induces neurotoxicity in Chinese rare minnows and reproductive toxicity in Japanese medaka (Hong et al., 2018; Li et al., 2018). Within zebrafish, TPHP induces neurotoxicity by altering neurotransmitter abundance and downregulating genes that regulate central

nervous system function (Shi et al., 2018) as well as impacts liver metabolism and function via alterations in glucose, UDP-glucose, lactate, succinate, fumarate, choline, acetylcarnitine, and several fatty acids (Du et al., 2016). Moreover, TPHP exposure causes thyroid endocrine disruption, ocular toxicity, cardiotoxicity, and hepatotoxicity (Du et al., 2016; Jarema et al., 2015; Kim et al., 2015; Liu et al., 2016; Mitchell et al., 2019; Shi et al., 2018, 2019). In zebrafish, TPHP alters the balance of sex hormones by altering estrogen metabolism or steroidogenesis (Liu et al., 2012; Yang et al., 2019) suggesting that TPHP may be an endocrine disruptor (Oliveri et al., 2015). TPHP also impacts the expression of transcriptional regulators (Yang et al., 2019), and developmental exposure has been found to result in long-term impairments on behavior (Oliveri et al., 2015; Yang et al., 2019).

Based on our prior studies, TPHP blocks cardiac looping during zebrafish embryogenesis in a concentration-dependent manner – an effect that is dependent on TPHP-induced fluid accumulation (edema) within the pericardial region enveloping the embryonic heart (Isales et al., 2015; Mitchell et al., 2018, 2019; Yozzo et al., 2013). As teleost (including zebrafish) embryos develop *ex utero*, mitochondria-rich epidermal ionocytes lining the embryonic skin express ion transporters and, as such, are responsible for maintaining an ionic/osmotic balance (osmoregulation) between the external aqueous environment and internal embryonic environment prior to the development of functional gills (Guh et al., 2015). Within freshwater fish, there are five types of aquaphilic ionocytes that regulate the uptake of ions through aquaporins and, as a result, control bodily fluids: KS (Potassium-Sodium pump), SLC (Sodium, Potassium, Chlorine, Bicarbonate pump), NCC (Sodium, Chlorine, Bicarbonate pump), NaRC (Calcium, sodium, potassium pump), and HR (Bicarbonate, sodium, hydrogen, carbon dioxide, ammonia, chlorine pump) (Kwong & Perry, 2015). Within zebrafish, epidermal ionocytes differentiate at

approximately 24 h post-fertilization (Hwang & Chou, 2013) and are derived from non-neural ectoderm which express ΔNp63 – a transcription factor that is required for epithelial cell proliferation (Jänicke et al., 2007). Following gastrulation, two specification markers for ionocytes – forkhead box I3a (Foxi3a) and Delta C, a ligand for Notch signaling – are expressed in ΔNp63-positive epidermal cells that differentiate into ionocyte progenitors (Hsiao et al., 2007; Jänicke et al., 2007). Notch signaling maintains cell fate after ionocyte progenitors progress through lateral inhibition by inhibiting Foxi3a expression. At the 14-somite stage, ΔNp63 expression in epidermal ionocyte progenitors is downregulated to allow Foxi3a-driven activation of ionocyte differentiation (Hsiao et al., 2007; Jänicke et al., 2007).

Despite our understanding about the role of ionocytes in osmoregulation, little is known about how environmental chemicals may impact the abundance and/or function of ionocytes within developing fish embryos. For example, exposure of larval zebrafish to cadmium results in a decrease in NaRC ionocytes, resulting in disruptions in Na^+ uptake (Dave & Kwong, 2020). Therefore, using zebrafish as a model, the objective of this study was to identify the potential role of epidermal ionocytes in mediating TPHP-induced pericardial edema formation within zebrafish embryos. To accomplish this objective, we relied on an ionocyte-specific antibody, whole-mount immunochemistry, and automated image acquisition/analysis protocols to quantify the number of epidermal ionocytes within developing zebrafish embryos. Moreover, we relied on mannitol (an osmotic diuretic) to determine whether an increase in the osmolarity of surrounding water mitigated or enhanced TPHP-induced effects on edema formation, ionocyte abundance, and the embryonic transcriptome.

Finally, we utilized morpholinos to knockdown ATPase1a1.4 – a Na^+/K^+-ATPase localized to epidermal ionocytes in zebrafish embryos – as well as ouabain – a broad-

spectrum Na^+/K^+-ATPase inhibitor – to determine whether the absence of functional ionocytes alters TPHP induced edema formation.

2.3 Materials and Methods

Animals

Using previously described procedures (Mitchell et al., 2018), adult wildtype (strain 5D) zebrafish were maintained and bred on a recirculating system according to an Institutional Animal Care and Use Committee-approved animal use protocol (#20180063) at the University of California, Riverside.

Chemicals

TPHP (99.5% purity) was purchased from ChemService, Inc. (West Chester, PA, USA); D mannitol (>98% purity) and ouabain (>95% purity) were purchased from Bio-Techne Corp. (Minneapolis, MN, USA). To prepare stock solutions, TPHP was dissolved in liquid chromatography-grade dimethyl sulfoxide (DMSO) and stored at room temperature in 2-mL glass amber vials with polytetrafluoroethylene-lined caps. To prepare working solutions, stock solutions of TPHP were spiked into particulate-free water from our recirculating system (pH and conductivity of ~7.2 and ~950 µS, respectively), resulting in 0.1% DMSO within all vehicle control and TPHP treatments. D-mannitol and ouabain solutions were freshly prepared by dissolving powder into particulate-free water from our recirculating system and then immediately used for exposures.

TPHP Exposures

Immediately after spawning, fertilized eggs were collected and incubated in groups of approximately 50 per 100 X 15 mm polystyrene petri dish until 24 h post-fertilization (hpf) within a light- and temperature-controlled incubator. Working solutions of vehicle (0.1% DMSO) or TPHP (2.5 µM, 5 µM, and 10 µM) were prepared as described above. Vehicle or TPHP solutions (10 mL) were added to 100 X 15 mm polystyrene petri

dishes and viable embryos were then transferred to dishes, resulting in 30 initial embryos per dish (three replicate dishes per treatment). Embryos were then exposed to vehicle or TPHP from 24 to 72 hpf. To determine the potential sensitive window of TPHP-induced impacts on ionocytes, embryos were exposed to vehicle (0.1% DMSO) or 5 μM TPHP from 24 to 72 hpf, 30 to 72 hpf, or 48 to 72 hpf. All dishes were covered with a lid and incubated under a 14-h:10-h light-dark cycle at 28ºC until 72 hpf. At 72 hpf, all embryos were then fixed overnight at 4ºC in 4% paraformaldehyde in 1X phosphate buffered saline (PBS), and then transferred to 1X PBS and stored at 4ºC for no longer than one month until whole-mount immunohistochemistry.

Whole-Mount Immunohistochemistry and Automated Imaging

Similar to previously described protocols (K. L. Yozzo et al., 2013), fixed embryos were labeled with a 1:10 dilution of a chicken ATPase1a1-specific antibody (a5-S) (Developmental Studies Hybridoma Bank, University of Iowa, Iowa City, IA, USA) and 1:500 dilution of AlexaFluor 488- conjugated goat anti-mouse IgG antibody (Thermo Fisher Scientific, Waltham, MA, USA) to quantify the abundance of embryonic ionocytes. Labeled embryos were transferred to black 384-well microplates containing 0.17-mm glass-bottom wells (Matrical Bioscience, Spokane, WA, USA), centrifuged for 5 min at 200 rpm, and imaged under transmitted light and a FITC filter on our ImageXpress Micro XLS Widefield High-Content Screening System within MetaXpress 6.0.3.1658 (Molecular Devices, Sunnyvale, CA, USA). Body length, pericardial area, and yolk sac area were manually quantified within MetaXpress using images captured under transmitted light, whereas ionocytes were automatically quantified with a custom module within MetaXpress using images captured under a FITC filter.

D-Mannitol and Ouabain Co-Exposures

Using procedures described above, embryos were exposed to either vehicle (0.1% DMSO), 5 μM TPHP, 250 mM D-mannitol, or 5 μM TPHP + 250 mM D-mannitol from 24 to 72 hpf. In addition, embryos were exposed to either vehicle (0.1% DMSO), 5 μM TPHP, 0.5 mM ouabain, or 5 μM TPHP + 0.5 mM ouabain from 24 to 72 hpf. At 72 hpf, embryos were fixed in 4% paraformaldehyde in 1X PBS overnight at 4ºC, and then transferred to 1X PBS and stored at 4ºC for no longer than one month until whole-mount immunohistochemistry.

Morpholino Injections

A custom lissamine-tagged, translational-blocking morpholino antisense oligo (MO) (Gene Tools, Inc., Philomath, OR, USA) was designed to target the ATPase Na+/K+ transporting subunit alpha 1a, tandem duplicate 4 (atp1a1a.4) (NCBI Gene ID: 64615; atp1a1a.4-MO sequence: 5'- ATTTCCAGTTCCAAGCCCCATTTTC-3'). ATPase1a1.4 was identified as a target for knockdown since 1) it's strongly expressed and colocalized with NaRCs within the embryonic skin of zebrafish, 2) the alpha subunits contain ion binding sites, 3) it predominates in freshwater fish (Liao et al., 2009; Esbaugh et al., 2019), and 4) it had high protein sequence homology with a chicken-specific ATPase1a. A lissamine-tagged negative control MO (nc-MO) (Gene Tools, Inc., Philomath, OR, USA) was used to account for potential non-target toxicity of MOs. Lyophilized MOs were resuspended in molecular biology-grade (MBG) water and MO stock solutions (1 mM) were stored in the dark at room temperature.

MO stock solutions were diluted in MBG water to prepare MO working solutions (0.5 mM). Similar to previously described methods (Cheng et al., 2019; Dasgupta et al., 2017; McGee et al., 2013), zebrafish embryos (1- to 8-cell stage) were microinjected with MOs (~3 nL per embryo) using a motorized Eppendorf Injectman NI2 and FemtoJet 4x.

MO delivery was confirmed at 3 hpf using a Leica MZ10 F stereomicroscope equipped with a DMC2900 camera and a RFP filter cube. Embryos that were non-fluorescent and/or coagulated were discarded. Fluorescent embryos were then exposed to either vehicle (0.1% DMSO) or 5 μM TPHP from 24 to 72 hpf and assessed for potential impacts on body length, pericardial area, yolk sac area, and ionocyte abundance as described above. To confirm knockdown of ATP1a1a.4, injected embryos (30 per dish; three replicate dishes per group) were fixed and labeled with a chicken ATPase1a1-specific antibody using whole-mount immunohistochemistry and imaging protocols described above.

mRNA-Sequencing

To quantify the potential for D-mannitol to mitigate or enhance TPHP-induced effects on the transcriptome, embryos were exposed to vehicle (0.1% DMSO), 250 mM D-mannitol, 5 μM TPHP, or 250 mM D-mannitol + 5 μM TPHP (30 embryos per dish; three replicates per treatment) from 24 to 72 hpf, transferred to 2-mL cryovials (three replicate pools per treatment) at 72 hpf, and then immediately snap-frozen in liquid nitrogen and stored at -80°C. Total RNA was extracted and libraries (12 total) were prepared following previously described methods (Cheng et al., 2019). With the exception of one treatment replicate from the D-mannitol-alone exposure, the remaining 11 libraries generated a sufficient number of reads passing filter for downstream analysis. Raw Illumina (fastq.gz) sequencing files (11 files) are available via NCBI's BioProject database under BioProject ID PRJNA751966. All 11 raw and indexed Illumina (fastq.gz) sequencing files were downloaded from Illumina's BaseSpace and analyzed within Bluebee (Lexogen Quantseq DE1.4) following previously described methods (Cheng et al., 2019).

Statistical Analyses

For phenotypic measurements (pericardial area, body length, yolk sac area, and ionocyte count), a general linear model (GLM) analysis of variance (ANOVA) (α=0.05) and Tukey-based multiple comparisons were performed using SPSS Statistics 24.

2.4 Results

TPHP increases ionocyte abundance following exposure from 24 to 72 hpf

Relative to embryos exposed to vehicle (0.1% DMSO) from 24 to 72 hpf, exposure to TPHP from 24 to 72 hpf resulted in significantly decreased body length at 5 and 10 μM TPHP; no significant effects on survival (>85%) (data not shown) nor yolk sac area at all concentrations tested (2.5, 5, and 10 μM); significantly increased pericardial area at 2.5, 5, and 10 μM TPHP; and significantly increased ionocyte abundance at 5 and 10 μM TPHP at 72 hpf (Figure 2.1). Therefore, we selected 5 μM TPHP as the optimal concentration for all subsequent experiments, as this was the lowest concentration that consistently increased pericardial area and ionocyte abundance following exposure from 24 to 72 hpf.

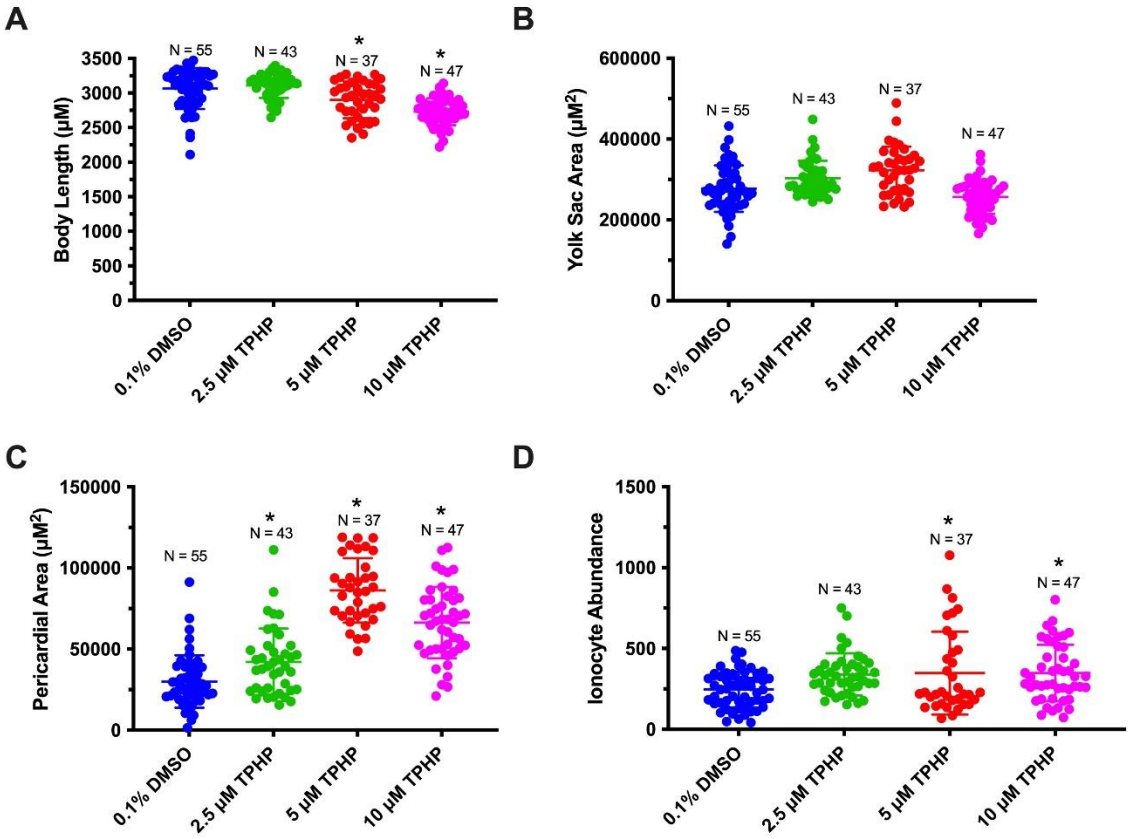

Figure 2.1. Mean (± standard deviation) of body length (A), yolk sac area (B), pericardial area (C) and ionocyte abundance (D) of embryos exposed to vehicle (0.1% DMSO), 2.5 µM TPHP, 5 µM TPHP, or 10 µM TPHP from 24-72 hpf. Asterisk (*) denotes significant difference (p<0.05) relative to vehicle (0.1% DMSO).

When exposures were initiated at 24 or 30 hpf, there was a significant decrease in body length; no effects on yolk sac area; and a significant increase in pericardial area within embryos to 5 µM TPHP relative to vehicle-exposed embryos at 72 hpf (Figure 2.2). While ionocyte abundance was significantly increased following exposure from 24 to 72 hpf, initiation of 5 µM TPHP exposure at 30 hpf mitigated TPHP-induced effects on ionocyte abundance at 72 hpf (Figure 2.2) even though the magnitude of TPHP-induced pericardial edema and body length effects were similar following exposure from 24 to 72 hpf and 30 to 72 hpf, suggesting that 1) 24-30 hpf represents a critical window of exposure for TPHP-induced effects on ionocyte abundance and 2) an increase in ionocyte

abundance may not be required for pericardial edema formation. When exposures were initiated at 48 hpf, the effects of 5 μM TPHP on body length, pericardial area, and ionocyte abundance were all significantly mitigated, suggesting that initiation of exposure prior to 48 hpf is required for TPHP-induced toxicity within zebrafish embryos.

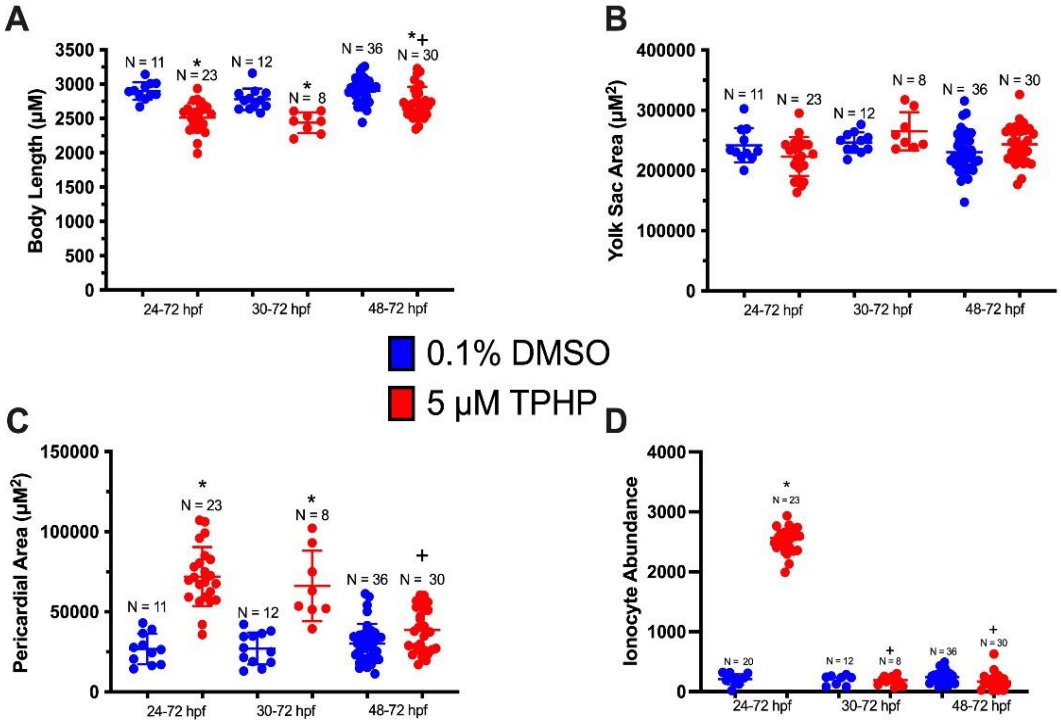

Figure 2.2. Mean (± standard deviation) of body length (A), yolk sac area (B), pericardial area (C) and ionocyte abundance (D) of embryos exposed to vehicle (0.1% DMSO) or 5 μM TPHP from 24- 72 hpf, 30-72 hpf or 48-72 hpf. Asterisk (*) denotes significant difference ($p < 0.05$) relative to vehicle (0.1% DMSO) within the same exposure scenario (24-72 hpf, 30-72 hpf or 48-72 hpf), whereas plus sign (+) denotes significant difference ($p<0.05$) relative to embryos exposed to 5 μM TPHP from 24-72 hpf.

D-Mannitol Mitigates TPHP-Induced Effects on Pericardial Area and Ionocyte Abundance

Embryos were exposed to 5 μM TPHP in the presence or absence of 250 mM D-mannitol from 24 to 72 hpf since TPHP-induced effects on ionocyte abundance only occurred following initiation of TPHP exposure at 24 hpf. Relative to embryos exposed to vehicle (0.1% DMSO) from 24 to 72 hpf, there was a significant decrease in body length following exposure to 5 μM TPHP or 5 μM TPHP + 250 mM D-mannitol; no effects on yolk

sac area across all treatment groups; and a significant increase in pericardial area and ionocyte abundance following exposure to 5 µM TPHP but not 5 µM TPHP + 250 mM D-mannitol (Figure 2.3).

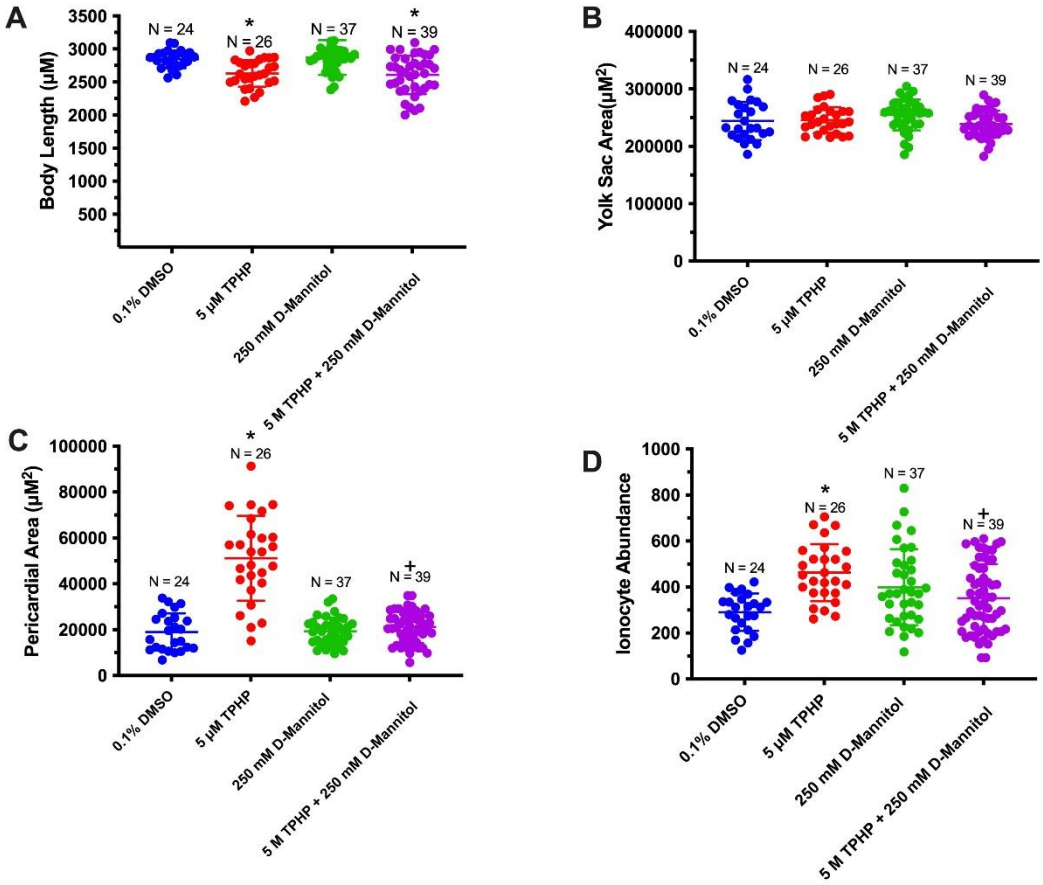

Figure 2.3. Mean (± standard deviation) of body length (A), yolk sac area (B), pericardial area (C) and ionocyte abundance (D) of embryos exposed to vehicle (0.1% DMSO), 5 µM TPHP, 250 mM D-Mannitol or 5 µM TPHP and 250 mM D-Mannitol from 24-72 hpf. Asterisk (*) denotes significant difference (p<0.05) relative to vehicle (0.1% DMSO), whereas plus sign (+) denotes significant difference (p<0.05) within the co-exposure relative to 5 µM TPHP alone.

Interestingly, exposure to 250 mM D-mannitol alone from 24 to 72 hpf resulted in significant impacts on the abundance of 417 transcripts (363 decreased and 54 increased) at 72 hpf (Figure 2.4) even though these embryos were phenotypically similar to vehicle-exposed embryos (Figure 2.3). Exposure to 5 µM TPHP from 24 to 72 hpf significantly impacted the abundance of five transcripts (four decreased and one increased) at 72 hpf

relative to vehicle-exposed embryos (Figure 2.4) – a finding that is consistent with our prior study (Mitchell et al., 2018) – and co-exposure to 5 µM TPHP + 250 mM D-Mannitol resulted in a significant impact on the abundance of 47 transcripts (25 decreased and 22 increased) at 72 hpf relative to relative to vehicle-exposed embryos (Figure 2.4).

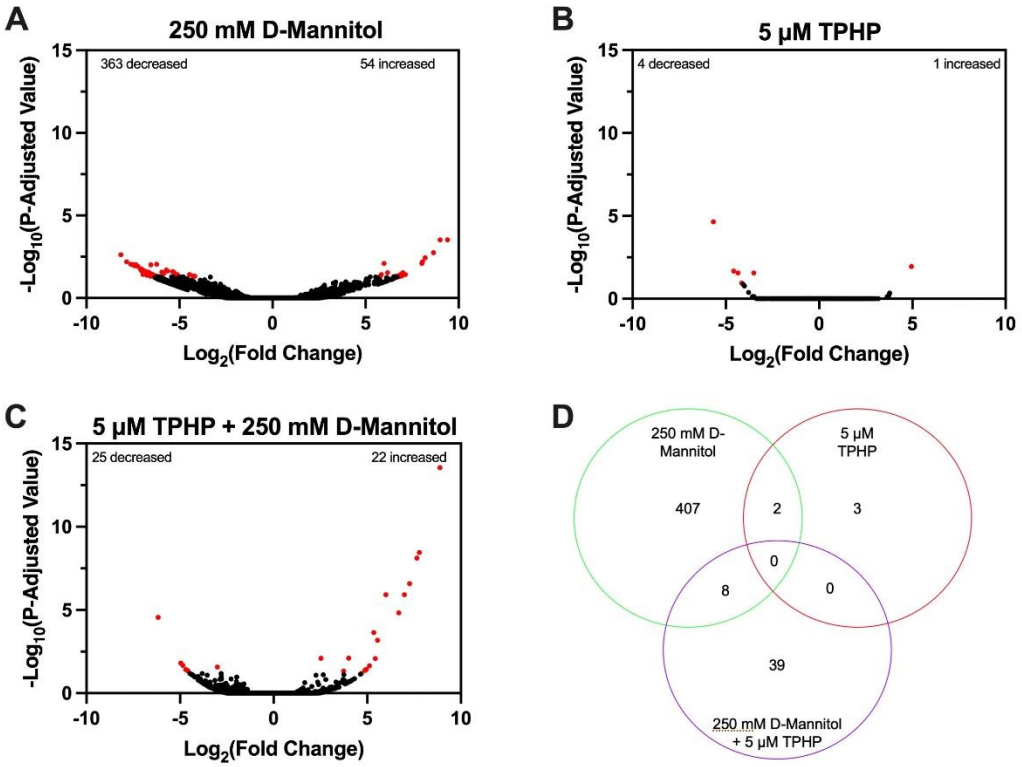

Figure 2.4. Volcano Plots showing the number of significantly different transcripts (red circles) following treatment with (A) 250 mM D-Mannitol (B) 5 µM TPHP, or (C) 5 µM TPHP and 250 mM D-Mannitol from 24-72 hpf relative to vehicle (0.1% DMSO). Log_2-transformed fold change is plotted on the x-axis and log_{10}- transformed-p-adjusted value is plotted on the x-axis log_{10}- transformed-p-adjusted value is plotted on the y-axis. Venn diagram showing the overlap of the transcripts among treatment groups (D).

ATPase1a1.4 Knockdown Mitigates TPHP-Induced Effects on Ionocyte Abundance Whereas Ouabain Enhances TPHP-Induced Effects on Pericardial Area

We were unable to confirm knockdown of ATPase1a1.4 *in situ* since 1) the ATPase1a1- specific antibody cross-reacts with cytosolic epitopes on the alpha subunit

of all Na^+/K^+-ATPase isoforms and 2) there are no commercially available antibodies that cross-react with zebrafish ATPase1a1.4. Nevertheless, we found that, relative to nc-MO-injected embryos, injection of ATPase1a1.4-MOs significantly mitigated the effects of 5 µM TPHP on ionocyte abundance – but not pericardial area – following exposure from 24 to 72 hpf (Figure 2.5). Interestingly, contrary to our findings following injection of ATPase1a1.4-MOs, we found that co-exposure of embryos to 5 µM TPHP + 0.5 mM ouabain from 24 to 72 hpf enhanced the effects of TPHP on pericardial area – but not ionocyte abundance – at 72 hpf (Figure 2.6).

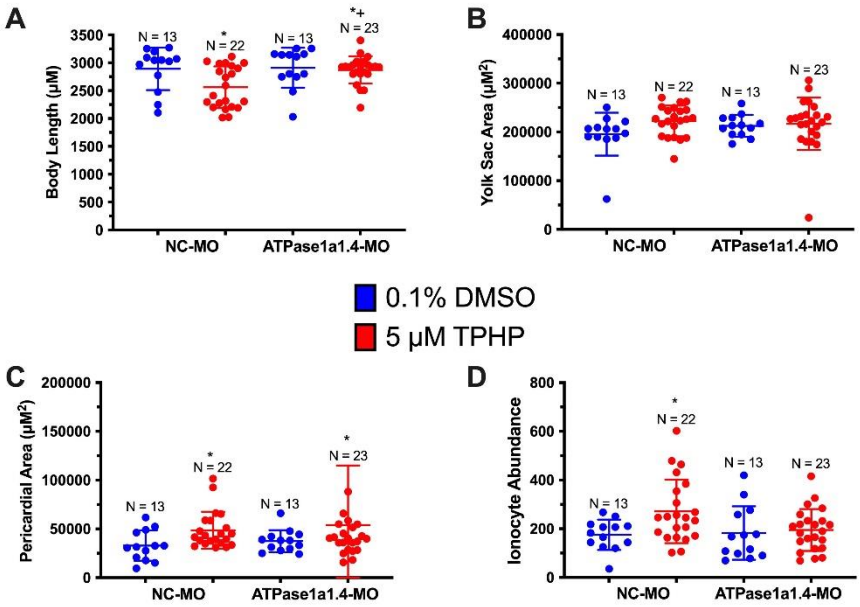

Figure 2.5. Mean (± standard deviation) of body length (A), yolk sac area (B), pericardial area (C) and ionocyte abundance following injection of nc-MOs or ATPase1a1.4-MO at 0.75 hpf and exposure from 24-72 hpf to vehicle (0.1% DMSO) or 5 µM TPHP. Asterisk (*) denotes a within-MO significant difference (p<0.05) relative to vehicle (0.1% DMSO), whereas plus sign (+) denotes a within treatment significant difference (p<0.05) relative to nc-MO-injected embryos.

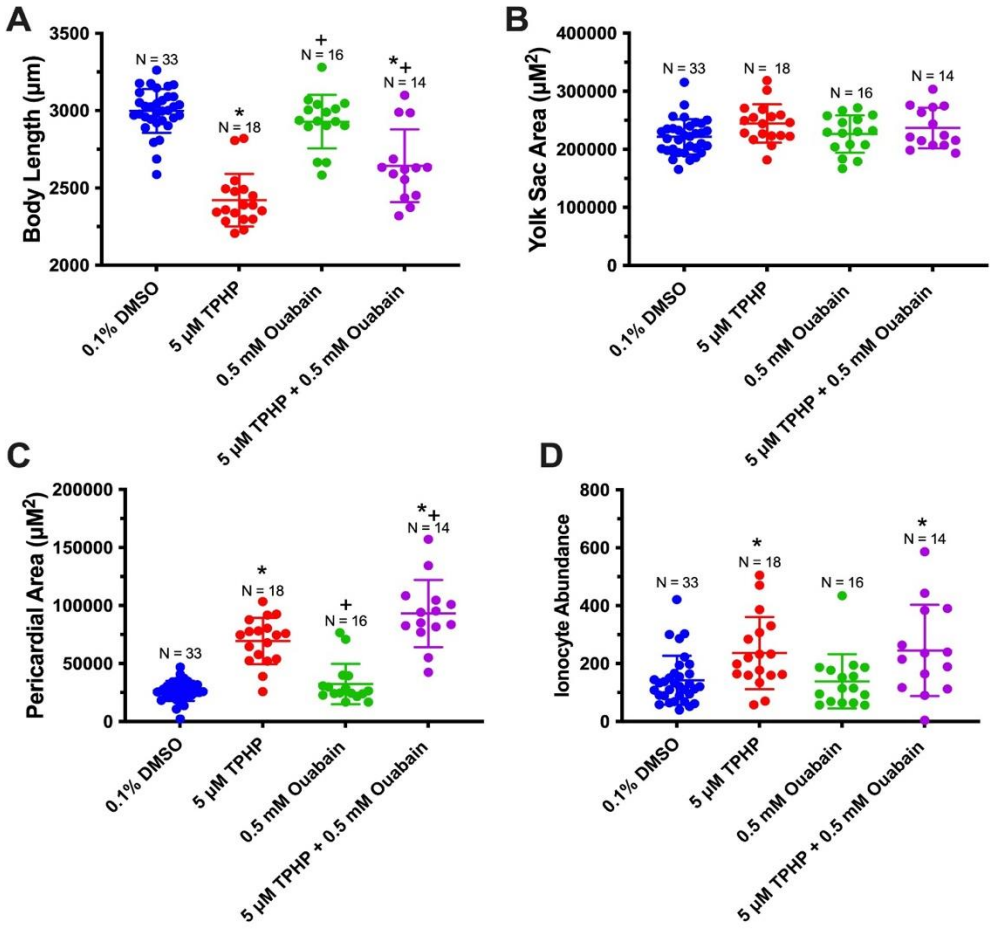

Figure 2.6. Mean (± standard deviation) of body length (A), yolk sac area (B), pericardial area (C) and ionocyte abundance following exposure of vehicle (0.1% DMSO), 5 µM TPHP, 0.5 mM Ouabain, or 5 µM TPHP + 0.5 mM Ouabain. Asterisk (*) denotes significant difference (p<0.05) relative to vehicle (0.1% DMSO), whereas plus sign (+) denotes significant difference (p<0.05) within the co-exposure relative to 5 µM TPHP alone.

2.5 Discussion

Based on our prior studies in embryonic zebrafish, TPHP is known to disrupt cardiac looping as well as induce pericardial edema and liver enlargement, effects that may be due to a disruption in osmotic balance and/or electrolyte/solute reabsorption (Isales et al., 2015; McGee et al., 2013; Mitchell et al., 2018; Reddam et al., 2019). Within this study, we identified a significant increase in Na+/K+ ATPase1a1-rich ionocytes (NaRCs) when zebrafish embryos were exposed to 5 µM TPHP from 24-72 hpf – an effect

that was associated with an increase in pericardial area and decreased body length similar to our past studies (Isales et al., 2015; McGee et al., 2013; Mitchell et al., 2018; Reddam et al., 2019). Moreover, we found that initiation of TPHP exposure at 24 hpf resulted in an increase in NaRC ionocytes in embryonic zebrafish whereas initiation of exposure at 30 and 48 hpf did not result in an increase in ionocyte abundance, suggesting that the sensitive window for a TPHP-induced increase in ionocytes was between 24 and 30 hpf. Contrary to our findings, a prior study found that cadmium exposure decreased the number of NaRC ionocytes within 72-hpf zebrafish (Dave & Kwong, 2020), suggesting that environmental contaminants may differentially impact the differentiation, proliferation, and/or survival of NaRC ionocytes within developing zebrafish embryos.

D-Mannitol is an osmoprotectant that has been used to mitigate 2,3,7,8-tetrachlorodibenzo p-dioxin (TCDD)-induced pericardial edema in developing zebrafish embryos (Antkiewicz et al., 2005; Hill et al., 2004). We previously found that D-mannitol was able to mitigate TPHP-induced pericardial edema (Mitchell et al., 2019), a finding that was likely driven by an increase in osmolarity of the surrounding water. Within this study, we found that co-exposure of embryos to D-mannitol similarly mitigated the effects of TPHP on pericardial area, suggesting that D-mannitol inhibited movement of water from outside to inside of the embryo following exposure to TPHP. Interestingly, based on our mRNA-sequencing data, exposure to D-mannitol alone or TPHP + D-mannitol resulted in significant impacts on the transcriptome (relative to TPHP-alone exposures) even though these embryos were phenotypically similar to vehicle-treated embryos, suggesting that D-mannitol – either in the presence or absence of TPHP – has the potential to affect transcription during embryonic development. Given that foxi3a and foxi3b are tightly regulated during zebrafish development (Hsiao et al., 2007), any alterations to these transcription factors caused by D mannitol may lead to changes in ionocyte abundance

and/or localization throughout the embryo. Indeed, similar to TPHP, exposure to D-Mannitol alone resulted in a slight increase (albeit non-significant) in the number of ionocytes.

Relative to nc-MO-injected embryos exposed to TPHP, knockdown of ATPase1a1.4 fully mitigated TPHP-induced effects on ionocyte abundance but not body length nor pericardial area, suggesting that the presence of ATPase1a1.4 is required for TPHP-induced effects on ionocyte abundance. Therefore, we used ouabain – a broad-spectrum Na^+/K^+-ATPase inhibitor – to determine whether the absence of functional ionocytes alters TPHP-induced effects on developing embryos (Shu et al., 2003). Contrary to the effects of ATPase1a1.4 knockdown, co-exposure to ouabain enhanced the impacts of TPHP on pericardial area, suggesting that inhibition of Na^+/K^+- ATPase exacerbates TPHP-induced edema formation and, contrary to D-mannitol, ouabain facilitated movement of water from outside to inside of the embryo following exposure to TPHP. Past studies have found that inhibiting ATPase1a leads to irregular heart rate in zebrafish embryos, and that inhibiting Na^+/K^+ ATPases leads to impaired cardiac development (Pott et al., 2018). Moreover, other studies that have found that Na^+ increases cortisol levels in zebrafish (Lin et al., 2016), and high cortisol levels have been linked to pericardial edema and increased heart deformities (Nesan & Vijayan, 2012). Therefore, if Na^+ increases inside the embryo, there is a possibility that cortisol levels may also increase, and drive TPHP-induced pericardial edema.

2.6 Conclusions

To our knowledge, this is one of the first studies to investigate the potential impacts of TPHP on ionocytes during early zebrafish development. Our data suggest that TPHP increases Na+/K+ ATPase1a1 abundance when exposure is initiated at 24 hpf, leading to potential impacts on osmoregulation and secondary effects on organ development.

Therefore, additional research is needed to determine if TPHP is impacting other ionocyte types and/or causing an imbalance in ion transport during embryonic development.

Chapter 3: Triphenyl Phosphate-Induced Pericardial Edema is Dependent on Media Ionic Strength and Disruption of the Embryonic Yolk Sac Epithelium

3.1 Abstract

Pericardial edema is a common phenotype observed in fish embryos following exposure to a wide range of contaminants. However, the mechanisms underlying chemically-induced pericardial edema remains unclear. One of the potential mechanisms underlying edema may be a disruption in osmoregulation. The objective of this study was to identify whether triphenyl phosphate (TPHP) – a widely used aryl phosphate ester-based flame retardant – induces pericardial edema via impacts ion transport and the skin of embryonic zebrafish. In addition to TPHP-induced effects on the morphology and organization on the embryonic yolk sac epithelium, an increase in ionic strength of exposure media exacerbated the impact of TPHP on pericardial edema when embryos were exposed from 24-72 h post-fertilization (hpf). However, there was no significant difference in embryonic sodium concentrations *in situ* compared to vehicle (0.1% DMSO) when exposed from 24-72 hpf. We also found that increasing the osmolarity of the exposure media with mannitol (an osmotic diuretic which mitigates TPHP-induced pericardial edema) and increasing the ionic strength of the exposure media (which exacerbates TPHP-induced pericardial edema) did not affect embryonic doses of TPHP, suggesting that TPHP uptake was not altered under these varying experimental conditions. Overall, our findings suggest that TPHP alters the structure of the epithelium of the yolk sac, leading to disruption on embryonic osmoregulation and pericardial edema formation.

3.2 Introduction

Pericardial edema – or fluid accumulation surrounding the developing heart – is an abnormal phenotype that is commonly observed across species of fish embryos following exposure to a wide range of structurally diverse chemicals (Duan et al., 2013; Hermsen et al., 2017; Hill et al., 2004; McCollum et al., 2017; McGruer et al., 2021; Yozzo et al., 2013). Depending on the magnitude and severity, pericardial edema has the potential to interfere with normal developmental landmarks leading to abnormalities such as cardiac looping defects, bradycardia, and kidney malformations (Hill et al., 2004; Isales et al., 2015; McGee et al., 2013; Mitchell et al., 2019; Yozzo et al., 2013). In zebrafish embryos, prior studies have suggested that edema is caused by kidney failure, circulatory failure, ionic imbalance, and permeability defects (Hill et al., 2004).

Zebrafish have emerged as a model teleost species to understand how embryonic and adult fish utilize osmoregulation to maintain homeostasis (Evans, 2011; Fridman, 2020; Hwang et al., 2011; Hwang & Chou, 2013; Kwong et al., 2014). As zebrafish do not have fully functional gills until approximately 14 days post fertilization (dpf), aquaporins and epidermal ionocytes play a critical role in maintaining homeostasis within the developing embryo and larvae (Guh et al., 2015). Within freshwater species, there are five types of ionocytes – KS (Potassium-Sodium pump), SLC (Sodium, Potassium, Chlorine, Bicarbonate pump), NCC (Sodium, Chlorine, Bicarbonate pump), NaRC (Calcium, Sodium, Potassium pump), and HR (Bicarbonate, sodium, hydrogen, carbon dioxide, ammonia, chlorine pump) (Guh et al., 2015) – that regulate uptake of potassium, sodium, chlorine, bicarbonate, hydrogen, carbon dioxide and ammonia through aquaporins which, in turn, regulate water exchange between the embryo and surrounding aqueous environment (Kwong & Perry, 2015). Within embryonic zebrafish, the skin is the primary site of osmoregulation prior to gill specific localization of ionocytes and aquaporins

at approximately 14 dpf (Guh et al., 2015). The skin of embryonic zebrafish also includes keratinocytes with distinct cell borders (Li et al., 2011), and ionocytes and aquaporins are localized throughout the epidermal layer along these cell borders (Li et al., 2011). Freshwater fish are dependent on the skin, kidney, and gills to maintain homeostasis as a result of being constantly surrounded by water that is necessary for survival. The skin creates a barrier for water and ions, while the kidney excretes water and organic waste (Serluca et al., 2002). Within zebrafish, these systems are critical within early life-stages since embryos primarily rely on oxygen diffusion from the surrounding water in order to survive (Pelster & Burggren, 1996). During development, a water permeability barrier consists of two separate barriers – one surrounding the embryonic body and one surrounding the yolk sac (Hagedorn et al., 1998) – which allows embryos to regulate water uptake in the absence of a chorion (Hill et al., 2004). Interestingly, prior studies have demonstrated that impaired maintenance of the barrier surrounding the embryonic body results in edema (Hill et al., 2004). The zebrafish embryonic yolk sac is made up of proteins (mostly vitellogenin) (Ge et al., 2017; Link et al., 2006) and lipids (cholesterol, phosphatidylcholine, and triglycerides) (Link et al., 2006). The yolk can bioaccumulate toxins from waterborne exposures (Chen et al., 2015; Choi et al., 2016; Dolgova et al., 2016; Souder & Gorelick, 2017), with uptake involving passive or active transport across the yolk sac epithelium (Sant & Timm-Laragy, 2018). The yolk sac epithelium contains a majority of ionocytes found in developing embryos, but there is little information about the function of epidermal ionocytes as well as susceptibility of epidermal ionocytes to environmental chemicals (Kwong et al., 2016; Sant & Timme-Laragy, 2018). The yolk sac is metabolically active (Cindrova-Davies et al., 2017), and due to its ability to bioaccumulate hydrophobic environmental chemicals, may alter the normal trajectory of the developing embryo (Sant & Timme-Laragy, 2018).

Our recent study found that pericardial edema was associated with elevated epidermal ionocytes within zebrafish embryos following a 24- to 72-hpf exposure to triphenyl phosphate (TPHP), an aryl phosphate ester-based flame retardant and plasticizer (Wiegand et al., 2022). Moreover, we found that co-exposure of embryos to mannitol (an osmotic diuretic) blocked TPHP induced pericardial edema and effects on ionocyte abundance, whereas knockdown of ATPase1a1.4 – an abundant Na^+/K^+-ATPase localized to epidermal ionocytes – mitigated TPHP-induced effects on ionocyte abundance but not pericardial edema. Overall, our study suggested that TPHP-induced toxicity during early stages of development may be driven by impacts on the osmoregulatory system within embryonic zebrafish (Wiegand et al., 2022). Therefore, the objective of this study was to identify whether TPHP impacts osmoregulation within embryonic zebrafish, and if disruption in osmoregulation is necessary for TPHP-induced pericardial edema. To accomplish this objective, we first utilized a fluorescent, sodium ion indicator dye and automated image acquisition/analysis protocols to quantify relative sodium concentrations *in situ*. Second, we utilized analytical chemistry to determine if the presence of mannitol or varying ionic strength of the surrounding exposure media affects TPHP uptake into the developing embryo. Third, we relied on ion chromatography and inductively coupled plasma optical emission spectrometry (ICP-OES) to quantify the concentrations of fluoride, chloride, nitrite, bromide, nitrate, phosphate, sulfate, sodium, calcium, potassium, and magnesium in different media used for embryo exposures, and how varying ion concentrations impact embryonic phenotypes. Finally, we utilized scanning electron microscopy to determine whether TPHP alters the morphology and/or organization of the yolk sac epithelium.

3.3 Materials and Methods

Animals

Using previously described procedures (Mitchell et al., 2018), wildtype adult (strain 5D) zebrafish were maintained and bred on a recirculating system according to an Institutional Animal Care and Use Committee-approved animal use protocol (#20210027) at the University of California, Riverside.

Chemicals

TPHP (99.5% purity) and D-mannitol (>98% purity) were purchased from ChemService, Inc. (West Chester, PA, USA) and Bio-Techne Corp. (Minneapolis, MN, USA), respectively. To prepare stock solutions, TPHP was dissolved in liquid chromatography-grade dimethyl sulfoxide (DMSO) and stored at room temperature in 2-mL glass amber vials with polytetrafluoroethylene-lined caps. To prepare working solutions, stock solutions of TPHP were spiked into particulate-free water from our recirculating system (pH and conductivity of ~7.2 and ~950 µS, respectively), resulting in 0.1% DMSO within all vehicle control and TPHP treatments. D-mannitol solutions were freshly prepared by dissolving powder into particulate-free water from our recirculating system and then immediately used for exposures.

TPHP Exposures

Immediately after spawning, fertilized eggs were collected and incubated in groups of approximately 50 per 100 X 15 mm polystyrene petri dish until 24 h post-fertilization (hpf) within a light- and temperature-controlled incubator. Working solutions of vehicle (0.1% DMSO) or TPHP (2.5 µM, 5 µM, and 10 µM) were prepared as described above. Vehicle or TPHP solutions (10 mL) were added to 100 X 15 mm polystyrene petri dishes and viable embryos were then transferred to dishes, resulting in 30 initial embryos per dish (three replicate dishes per treatment). Embryos were then exposed to vehicle or

TPHP from 24 to 72 hpf. All dishes were covered with a lid and incubated under a 14-h:10-h light-dark cycle at 28ºC until 72 hpf. At 72 hpf, embryos were either 1) fixed overnight at 4ºC in 4% paraformaldehyde in 1X phosphate buffered saline (PBS), transferred to 1X PBS, and stored at 4ºC for no longer than one month until imaging or 2) immediately stained and analyzed for embryonic sodium concentrations as described below.

Quantification of Embryonic Sodium Concentrations

At 72 hpf, embryos were stained with a fluorescent sodium indicator dye (CoroNa Green AM, Invitrogen, Waltham, MA, USA) to quantify embryonic sodium concentrations *in situ*. At 72 hpf, the embryos were rinsed three times with reverse osmosis (RO) water and then placed in a working solution containing RO water, 20% Pluronic F-127 (Invitrogen, Waltham, MA, USA), and CoroNa Green AM for 1.5 h. The working solution was then aspirated, and embryos were washed with RO water another three times for 5 min each. Finally, embryos were immobilized with 100 mg/L MS 222 for 3 min, transferred into 96-well plates, and imaged under transmitted light and a FITC filter on our ImageXpress Micro XLS Widefield High-Content Screening System within MetaXpress 6.0.3.1658 (Molecular Devices, Sunnyvale, CA, USA). Body length, pericardial area, and yolk sac area were manually quantified within MetaXpress using images captured under transmitted light, whereas total area of sodium-derived fluorescence in the head, trunk and yolk sac was quantified with a custom module within MetaXpress using images captured under a FITC filter.

Embryo Media Experiments

Different concentrations (0.5X, 1X and 2X) of embryo media (EM) were created by diluting a stock concentration of 60X EM within RO water. 60X EM was made in-house by dissolving 17.2 g NaCl, 0.76 g KCl, 2.9 g $CaCl_2 \cdot 2H_20$, and 4.9 g $MgSO_4 \cdot 7H_20$ into 1 L

of RO water, and then autoclaving the final solution prior to long-term storage at 4°C. Varying concentrations of EM were used for TPHP exposures by spiking DMSO or TPHP in 0.5X, 1X or 2X EM, resulting in a final concentration of either 0.1% DMSO or 5 μM TPHP. Immediately after spawning, fertilized eggs were collected and incubated in groups of approximately 50 per 100 X 15 mm polystyrene petri dish until 24 hpf within a light- and temperature-controlled incubator. Working solutions of vehicle (0.1% DMSO) or 5 μM TPHP in EM (0.5X, 1X or 2X) were prepared as described above. Vehicle or TPHP solutions (10 mL) were added to 100 X 15 mm polystyrene petri dishes and viable embryos were then transferred to dishes, resulting in 30 initial embryos per dish (three replicate dishes per treatment). Embryos were then exposed to vehicle or TPHP from 24 to 72 hpf. All dishes were covered with a lid and incubated under a 14-h:10-h light-dark cycle at 28ºC until 72 hpf. At 72 hpf, all embryos were analyzed for embryonic sodium concentrations as described above.

EM Ingredient Experiments

To determine if one of the EM ingredients was necessary for TPHP-induced pericardial edema, exposures of TPHP were performed in four different solutions containing individual ingredients of 2X EM. Four different solutions were prepared in RO water: 10 mM NaCl, 0.17 mM KCl, 0.66mM $CaCl_2 \cdot 2H_20$, or 0.66mM $MgSO_4 \cdot 7H_20$. Each of these solutions were then spiked with DMSO or TPHP, resulting in a final concentration of either 0.1% DMSO or 5 μM TPHP. Embryos were then exposed from 24-72 hpf as described above. At 72 hpf, all embryos were analyzed for embryonic sodium concentrations as described above.

Quantification of Embryonic Doses of TPHP and DPHP

Embryonic doses of TPHP and diphenyl phosphate (DPHP, the primary metabolite of TPHP) were quantified following exposure to TPHP from 24-72 hpf in RO water, system

water, or 2X EM as described above. For the first experiment, 24-hpf embryos were transferred to 100 X 15 mm polystyrene Petri dishes (30 embryos per dish; four dishes per treatment) containing either system water and 0.1% DMSO, 5 μM TPHP, 250 mM D-Mannitol, or 5 μM TPHP + 250 mM D-Mannitol. For the second experiment, 24-hpf embryos were transferred to 100 X 15 mm polystyrene Petri dishes (30 embryos per dish; four dishes per treatment) containing either 1) RO water + 0.1% DMSO or 5 μM TPHP, or 1) 2X EM + 0.1% DMSO or 5 μM TPHP. All embryos were incubated until 72 hpf. For each replicate group (4 groups per treatment), ~30 embryos were placed into a 2-mL cryovial, immediately snap-frozen in liquid nitrogen, and stored at -80°C. Prior to extraction, samples were spiked with deuterated TPHP (d15-TPHP) and deuterated DPHP (d10-DPHP). Analytes were extracted and quantified similar to previously published methods (Mitchell et al., 2018). Method detection limits (MDLs) were set as three times the standard deviation of lab blanks (if present) or three times the noise. The MDLs for DPHP and TPHP were 0.86 ng and 1.19 ng, respectively, for the first experiment, and 0.50 ng. and 0.032 ng, respectively, for the second experiment.

Ion Chromatography and ICP-OES

To determine the concentration of ions within water being used in our experiments, 10 mL samples of RO, system water, 0.5X EM, 1X EM, and 2X EM were analyzed within UCR's Environmental Science Research Laboratory. Anions of interest were analyzed using a Dionex AQUION (Sunnyvale, CA) model ion chromatograph (IC) fitted with a conductivity cell detector, a 10-μL sample injection loop, Ion Pac AG14 (4x80 mm), AS14 (4x250 mm) guard and analytical columns maintained at 30°C, DRS-600 (4 mm) self-regenerating suppressor, and DV40 autosampler. The resin composition was ethylvinylbenzene cross-linked with divinylbenzene. The column specifications were the following: 9-μm particle size, 55% substrate crosslinking, anion exchange capacity of 65

μeq, alkyl quaternary ammonium ion exchange group, and medium-high hydrophobicity. Calibration standards were diluted from certified stock solutions using deionized water prepared via a Labconco WaterPro DS system (Kansas City, MO). Eluent was prepared using this deionized water with the following concentration: 3.5mM Na2CO3/1.0 mM NaHCO3. All glassware was washed using this deionized water. Anions were calibrated using concentrations ranging from 0.01 to 1000 ppm, with a limit of detection (LOD) determined using the equation LOD = (3.3 x $SD_{y\text{-intercept}}$)/slope. Verification of calibration efficacy was conducted by analysis of a certified multi-anion reference standard, “VeriSpec Mixed Anion Standard 7”, yielding percent recoveries from 91% to 99% for all seven anions.

Cations were analyzed utilizing an Optima 7300 DV Model Inductively Coupled Plasma – Optical Emission Spectrometer (ICP-OES, Perkin-Elmer, Waltham, MA) and using an Elemental Scientific (Omaha, NB) 4DXC autosampler. Samples and standards were pumped into a nebulization spray chamber at a rate of 0.80 mL per minute. These aerosolized droplets of 10 μm in diameter were then drawn into the argon plasma via a gas pressure of 0.5 L per min. The carrier liquid was 1% trace metal grade nitric acid (HNO_3), and a mixing T provided an inflow of 2.5 ppm Yttrium to serve as an internal standard. The argon plasma was generated using a gas flow rate of 14 L per min and a radio frequency inducement of 1350W. Auxiliary gas flow was set to 0.2 L per min. Calibration standards were diluted from stock solutions certified by Spex, using deionized water prepared via a Labconco WaterPro DS system (Kansas City, MO) and trace metal grade nitric acid. Polypropylene flasks were used for all liquid preparations. Cations were calibrated using concentration ranging from 0.01 to 1000 ppm, with limit of detection (LOD) determined using the equation LOD = (3.3 x $SD_{y\text{-intercept}}$)/slope. Verification of calibration efficacy was conducted by analysis of a certified multi-anion reference

standard prepared by VWR, yielding percent recoveries from 89% to 99% for all four cations.

Scanning Electron Microscopy

To determine if TPHP induced alterations to the yolk sac epithelium, a Hitachi Tabletop TM4000Plus Scanning Electron Microscope (SEM) was utilized to scan five independent locations on the yolk sac of each embryo. Prior to imaging, exposures were performed from 24-72 hpf within RO water, system water, or 2X EM containing 0.1% DMSO, 5 µM TPHP, 250 mM D-Mannitol, or 5 µM TPHP + 250 mM D-Mannitol. At 72 hpf, all embryos were fixed within 4% PFA as described above. Immediately before imaging, fixed embryos were flash frozen within a liquid nitrogen bath. Frozen embryos were then imaged using the following magnification and settings: 10 KV, setting 4, VSE, 2,000 X. Images were then analyzed within ImageJ (Version 1.8.0_172) using the following steps:

1. File → Open → Chose photo for analysis.
2. Choose *straight* line button on the toolbar and measure one side of the well to the other. Then chose Analyze → Set Scale (keep distance listed in pixels the same, make known distance 3, keep the pixel aspect ratio the same, Unit length is mm, and click the checkbox next to global).
3. Image → Adjust → Threshold (set first box to 0 and second box to 35) → click apply.
4. Analyze → Analyze particles (make sure the box next to summary is clicked).
5. The number under total area provides the total area of microridges in the image, record, and repeat steps.

Statistics

For all data generated within this study, a general linear model (GLM) analysis of variance (ANOVA) ($\alpha = 0.05$) and Tukey-based multiple comparisons were performed using SPSS Statistics 24.

3.4 Results

TPHP Does not Affect Embryonic Sodium Concentrations In Situ

Relative to embryos exposed to vehicle (0.1% DMSO) from 24-72 hpf, exposure to TPHP (2.5 μM, 5 μM and 10 μM) from 24-72 hpf did not significantly affect sodium concentrations within the head, yolk sac or trunk of embryonic zebrafish (Figure 3.1). Pericardial edema and yolk sac area were also quantified and, consistent with our prior studies, we found no significant differences in the yolk sac area whereas TPHP increased pericardial area in a concentration-dependent manner (Figure 3.1).

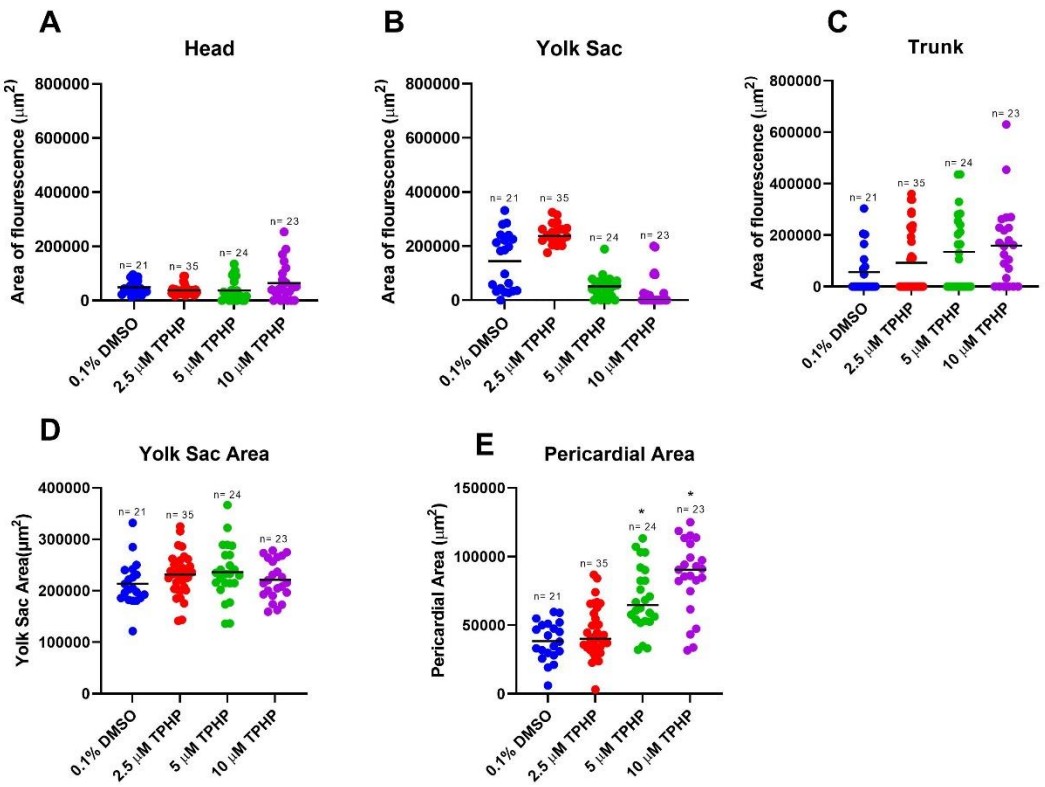

Figure 3.1. Mean (± standard deviation) of the area of fluorescence in the head (A), yolk sac (B), trunk (C), total area of the yolk sac (D), and pericardial area (E) of embryos exposed to vehicle (0.1% DMSO), 2.5 µM TPHP, 5 µM TPHP or 10 µM TPHP from 24-72 hpf. Asterisks (*) denotes a significant difference ($p<0.05$) relative to vehicle controls.

TPHP-Induced Pericardial Edema is Dependent on Ionic Strength Within Exposure Media

To better characterize the ionic composition of exposure media used within this study, we first quantified the concentration (in ppm) of Fluoride, Chloride, Nitrite, Bromide, Nitrate, Phosphate, Sulfate, Sodium, Calcium, Potassium, or Magnesium in RO Water, System Water, 0.5X EM, 1X EM, and 2X EM. While certain ions were present within System Water, 0.5X EM, 1X EM, and 2X EM but not RO Water, the concentration of chloride increased as a function of EM strength and accounted for the majority of ions present within 0.5X, 1X, and 2X EM (Figure 3.2). Indeed, the concentration of chloride

within 2X EM was 3X higher than the next highest ion (sodium) (Figure 3.2), a finding that was not surprising since three out of the four salts used to make EM contain chloride.

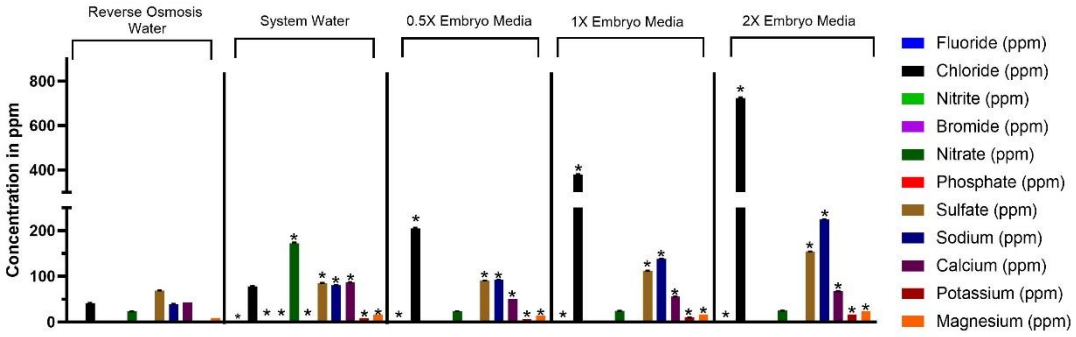

Figure 3.2. Mean (± standard deviation) of the concentration (in ppm) of Fluoride, Chloride, Nitrite, Bromide, Nitrate, Phosphate, Sulfate, Sodium, Calcium, Potassium, or Magnesium in RO Water, System Water, 0.5X EM, 1X EM, and 2X EM. Asterisks (*) denotes a significant difference ($p<0.05$) relative to RO water.

Embryos were exposed to 5 μM TPHP in different exposure media (RO Water, 0.5X EM, 1X EM, or 2X EM) from 24-72 hpf to determine if an increase in ionic strength of exposure media altered TPHP-induced pericardial edema. While TPHP decreased body length across all exposure media, TPHP did not affect yolk sac area within any of exposure media (Figure 3.3). However, we found that, even in the presence of TPHP, pericardial area was not significantly different from water or vehicle controls when exposed within RO water or 0.5X EM (Figure 3.3). However, when embryos were exposed to TPHP within 1X or 2X EM, pericardial area was significantly higher relative to water and vehicle controls, similar to what we have observed in this study and our prior studies using system water (Figure 3.3).

Interestingly, similar to our prior findings in system water, D-Mannitol completely mitigated TPHP-induced pericardial edema within co-exposed within 1X or 2X EM (Figure 3.3).

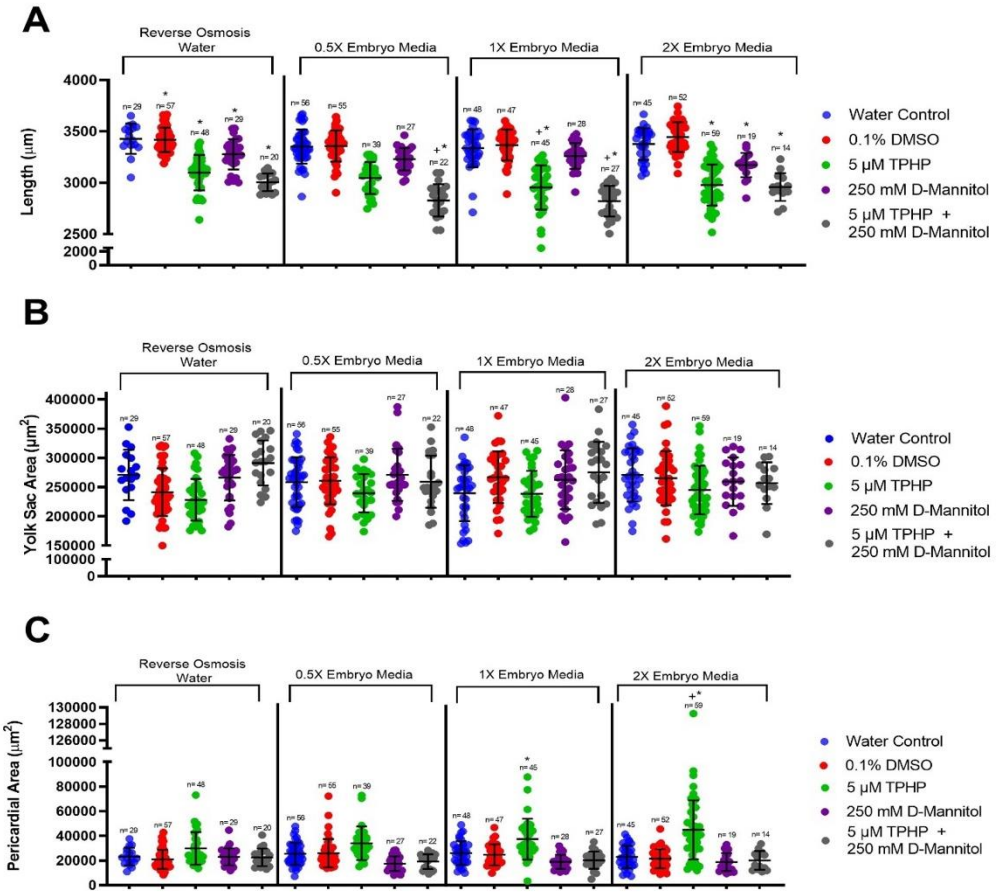

Figure 3.3. Mean (± standard deviation) of length (A), yolk sac area (B) and pericardial area (C) of embryos exposed to water control, vehicle (0.1% DMSO), 5 µM TPHP, 250 mM D-Mannitol, or 5 µM TPHP + 250 mM D-Mannitol in different types of media (RO Water, 0.5X EM, 1X EM, or 2X EM. Plus sign (+) denotes a significant difference ($p<0.05$) relative to 5 µM TPHP in RO water, whereas an asterisk (*) denotes a significant difference ($p<0.05$) relative to embryos exposed to vehicle (0.1% DMSO) within the same media group (RO Water, 0.5X EM, 1X EM or 2X EM).

To determine if a specific salt within EM was required for TPHP-induced pericardial edema, each EM ingredient was tested individually by exposing embryos to either vehicle (0.1% DMSO) or 5 μM TPHP. While there were no significant differences in body length or yolk sac area across all groups, pericardial area was significantly increased when embryos were exposed to TPHP within exposure media containing any of four EM ingredients (Figure 3.4). Interestingly, the most significant effects were observed when embryos were exposed within exposure media containing KCl, $CaCl_2 \bullet 2H_2O$, or NaCl, suggesting that chloride may be playing a key role in pericardial edema formation.

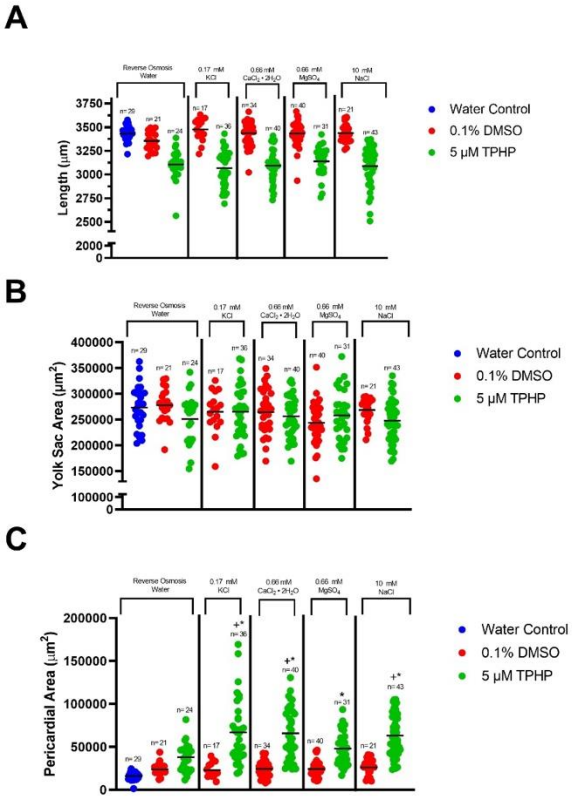

Figure 3.4. Mean (± standard deviation) of length (A), yolk sac area (B), and pericardial area (C) of embryos exposed to water control, vehicle (0.1% DMSO) or 5 μM TPHP in varying exposure media (10.18 mM KCl, 19.73 mM $CaCl_2 \bullet 2H_2O$, 40.71 mM $MgSO_4$, and 294.3 mM NaCl). Asterisks (*) denotes a significant difference ($p<0.05$) relative to vehicle (0.1% DMSO) in the same exposure media group (0.17 mM KCl, 0.66 mM $CaCl_2 \bullet 2H_2O$, 0.66 mM $MgSO_4$, and 10 mM NaCl), whereas a plus sign (+) denotes a significant difference ($p<0.05$) relative to embryos exposed to 5 μM TPHP in RO Water.

D-Mannitol and ionic strength of exposure media do not impact TPHP uptake.

Since D-mannitol (an osmotic diuretic) mitigates TPHP-induced pericardial edema and increasing the ionic strength of exposure media exacerbates TPHP-induced pericardial edema, we quantified embryonic doses of TPHP and DPHP in the presence of D-mannitol or within RO Water vs. 2X EM. Interestingly, embryonic doses of TPHP and DPHP were not affected by the presence of D-mannitol nor significantly different within RO Water vs. 2X EM (Figure 3.5), suggesting that differences in the severity of TPHP-induced pericardial edema under these varying experimental conditions were not attributed to differences in TPHP uptake.

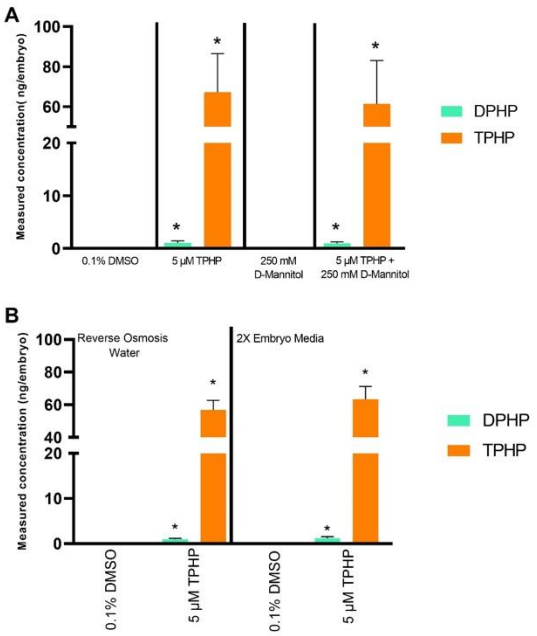

Figure 3.5. A) Mean (± standard deviation) of measured concentration of DPHP and TPHP (ng/embryo) in embryos exposed to vehicle (0.1% DMSO), 5 µM TPHP, 250 mM D-Mannitol, and 5 µM TPHP + 250 mM D-Mannitol from 24-72 hpf. Asterisks (*) denotes a significant difference ($p<0.05$) relative to vehicle (0.1% DMSO). B) Mean (± standard deviation) of measured concentration of DPHP and TPHP (ng/embryo) in embryos exposed to vehicle (0.1% DMSO) or 5 µM TPHP in different medias (RO Water or 2X EM). Asterisks (*) denotes a significant difference ($p<0.05$) relative to vehicle (0.1% DMSO).

TPHP Disrupts the Morphology and Organization of the Embryonic Yolk Sac Epithelium

Overall, TPHP-exposed in 2X embryo media embryos exhibited extensive microridges relative to embryos exposed to vehicle in Location C and E (Figure 3.6). While microridges in TPHP exposed embryos were higher at all locations, we only observed significant differences in those three locations. Embryos exposed to TPHP within 2X EM also exhibited extensive microridges relative to TPHP-exposed embryos in RO water at Locations C and E (Figure 3.6). Interestingly, in all but one of the locations, embryos exposed to both TPHP and D-Mannitol within 2X EM had significantly less microridges compared to embryos exposed to TPHP alone (Figure 3.6). At all 5 locations, there is also an upward trend in the abundance of microridges observed within TPHP exposed embryos, suggesting that an increase in ionic strength of exposure media exacerbated the generation of microridges within embryos.

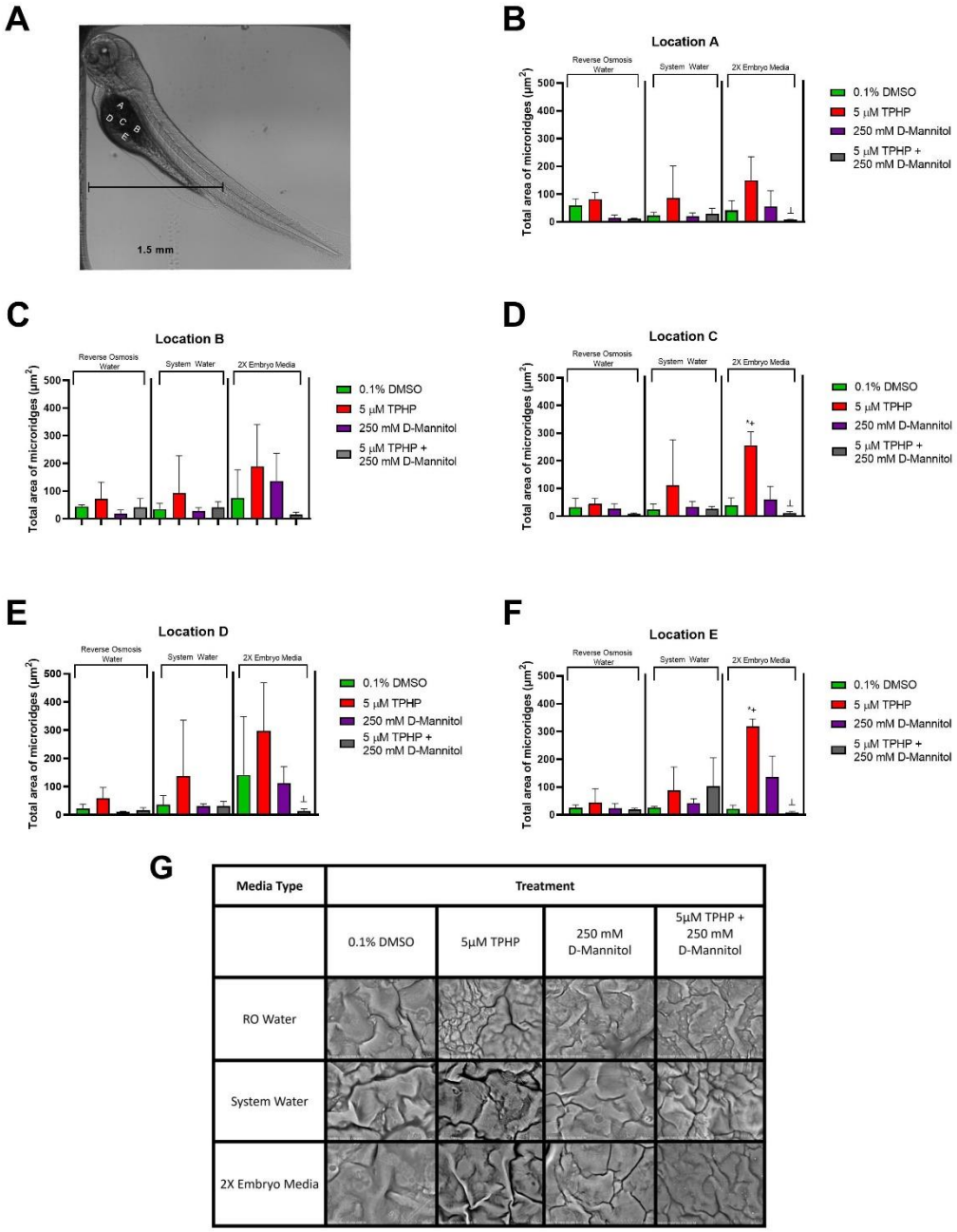

Figure 3.6. Locations (A, B, C, D, and E) used for SEM on the yolk sac of embryonic zebrafish (A). Panels B-F show the total area of microridges across treatment groups within each location. (G) Representative images of Location C are shown. * denotes a significant difference ($p<0.05$) relative to vehicle (0.1% DMSO) within same exposure media. + denotes a significant difference ($p<0.05$) relative to 5 μM TPHP in RO Water. ⊥ denotes a significant difference ($p<0.05$) relative to 5 μM TPHP in 2X EM.

3.5 Discussion

Based on our prior studies in developing zebrafish, TPHP is known to increase the number of ionocytes, as well as induce pericardial edema, liver enlargement and disrupt cardiac looping (Isales et al., 2015; McGee et al., 2013; Mitchell et al., 2018; Reddam et al., 2019; Wiegand et al., 2022). Within this study, we found that TPHP-induced pericardial edema is dependent on the presence of high ion concentrations within exposure media – a result that was likely associated with pericardial edema, increased ionocytes, and decreased body length found in our last studies (Isales et al., 2015; McGee et al., 2013; Mitchell et al., 2018; Reddam et al., 2019; Wiegand et al., 2022; Yozzo et al., 2013). Numerous studies have shown how changing the ion concentration of media can impact embryonic development (Liao et al., 2009; Esaki M et al., 2009; Esbaugh et al., 2019). However, to our knowledge, little is known about how ionic strength of exposure media impacts the toxicity of chemicals within zebrafish embryos. Indeed, our findings have significant implications due to minimal standardization of zebrafish embryo-based toxicity assays around the world.

We also found that TPHP altered the structure of the embryonic yolk sac epithelium by inducing an increase in the presence of microridges. This difference was more pronounced within TPHP-exposed embryos in 2X EM, where the yolk sac epithelium of TPHP-exposed embryos exhibited significantly more microridges relative to vehicle-exposed embryos in the same exposure media as well as TPHP-exposed embryos within RO water. This TPHP-induced phenotype was different from D-Mannitol and co-exposure groups, which consistently had the lowest amounts of microridges in all five locations. To our knowledge, only one other study has investigated the potential impacts of contaminants on the epithelium of embryonic zebrafish.

This study found that metal oxide nanoparticles caused skin damage on embryonic zebrafish (Peng et al., 2018) but, unlike our study, most of the skin damage was localized to the posterior regions.

Most studies in the published literature have investigated the epithelial layer of adult rather than embryonic zebrafish. Interestingly, these studies have looked at the capacity for cutaneous wound healing within zebrafish (Naomi et al., 2021) and, as such, are difficult to compare to our results due to differences of the epithelial layer of adult vs. embryonic zebrafish. For example, embryonic zebrafish utilize the entire epithelial layer for osmoregulation due to ionocytes and aquaporins being spread across their skin, while adult zebrafish have ionocytes and aquaporins localized to their gills, which occurs around 14 dpf (Breves et al., 2014; Dymowska et al., 2012; Evans, 2008, 2011; Gilmour, 2012; Hiroi & McCormick, 2012; Hwang & Lee, 2007; Hwang et al., 2011; Kumai & Perry, 2012; Wright & Wood, 2012). Embryonic zebrafish also do not develop scales until around 30 dpf (Le Guellec et al., 2003), making the embryonic skin more vulnerable to damage that may not impact adult zebrafish.

There are potential explanations underlying how TPHP-induced damage may be occurring. First, there may be an impact on the differentiation of ionocytes and/or keratinocytes. This disruption may be causing more ionocytes of different types to be produced, which was seen in our recent study (Wiegand et al., 2022). Second, there may be alterations in the maintenance of tight-junction barriers between keratinocytes (Kiener et al., 2008), alterations which have been found to cause similar phenotypes as TPHP-induced effects in zebrafish embryos. Interestingly, weakening of tight junctions on the epithelium as a result of toxin exposure has the potential to cause defects in osmoregulation (Hill et al., 2004; Kiener et al., 2008). On the yolk sac epithelium layer, tight-junction proteins regulate the paracellular movement of ions and fluids, with claudins

being the primary determinant of the epithelial barrier function (Guh et al., 2015; Turksen & Troy, 2004).

3.6 Conclusions

To our knowledge, this is the first study to investigate the potential impacts of TPHP on the embryonic yolk sac epithelium during early zebrafish development, and how changing ion composition of exposure media impacts the toxicity of TPHP within zebrafish embryos. Our data suggests that TPHP increases the frequency of microridges on the embryonic yolk sac epithelium, leading to potential impacts on osmoregulation and organ development during embryogenesis. We also found that changing the ionic strength of exposure media influenced the severity of pericardial edema formation, with increased ionic strength of the exposure media leading to increased pericardial edema. We also demonstrated that D-Mannitol does not impact TPHP uptake in embryonic zebrafish while still preventing TPHP-induced pericardial edema formation. Further research is needed to determine if TPHP is impacting the ability of embryonic zebrafish to repair its epithelial layer, leading to an imbalance in ion transport during embryonic development.

Chapter 4: Triphenyl Phosphate-Induced Pericardial Edema in Zebrafish: Role of Epidermal Injury and Uptake/Depuration Kinetics During Embryonic Development

4.1 Abstract

Triphenyl phosphate (TPHP) – a widely used organophosphate-based flame retardant – blocks cardiac looping during zebrafish development in a concentration-dependent manner, a phenotype that is dependent on disruption of embryonic osmoregulation and pericardial edema formation. However, it's currently unclear whether 1) TPHP-induced effects on osmoregulation are driven by direct, TPHP-induced injury to the embryonic epidermis and 2) whether TPHP-induced pericardial edema is reversible or irreversible following cessation of exposure. Therefore, the objectives of this study were to determine whether TPHP-induced pericardial edema is reversible, and whether TPHP causes injury to the embryonic epidermis by quantifying the number of DAPI-positive epidermal cells and analyzing the morphology of the yolk sac epithelium using scanning electron microscopy. First, we found that exposure to TPHP from 24-72 h post-fertilization (hp) did not increase prolactin – a hormone that regulates ions and water levels – in embryonic zebrafish, whereas high ionic strength exposure media was associated with elevated levels of prolactin. Second, we found that TPHP did not decrease DAPI-positive epidermal cells within the embryonic epithelium, and that fenretinide – a synthetic retinoid that promotes epithelial wound repair – partially mitigated the prevalence of TPHP-induced microridges within the yolk sac epithelium. Finally, we found that the pericardial area of TPHP-exposed embryos was similar to vehicle-treated embryos following transfer to clean water and depuration of TPHP. Overall, our findings suggest that 1) TPHP does not cause injury to the embryonic epidermis; 2) TPHP-induced pericardial edema is reversible; and

3) the ionic strength of exposure media has the potential to influence the baseline physiology of zebrafish embryos.

4.2 Introduction

Fish maintain ionic and osmotic homeostasis to ensure optimal cellular and physiological processes (Guh et al., 2015). Similar to humans, this process is achieved by utilizing transepithelial transport mechanisms (Guh et al., 2015). However, unlike humans, fish regulate ionic and osmotic gradients between an external aquatic environment and internal biological system (Guh et al., 2015). Osmoregulation has evolved to quickly adapt to changes in the aquatic environment, which can vary in osmolarity and ionic composition (Guh et al., 2015). Adult fish perform many ionic and osmoregulatory mechanisms within the gills, which have a similar role as the human kidney (Evans, 2008; Hwang & Lee, 2007). Within the gills, ionocytes represent major, mitochondria-rich cells that are responsible for the transport of ions and are functionally analogous to mammalian renal tubular cells (Dymowska et al., 2012; Evans, 2011; Guh et al., 2015; Hwang et al., 2011).

After fertilization of zebrafish eggs, ionocytes begin to differentiate at approximately 24 h post-fertilization (hpf) and are localized along the embryonic skin (or epidermis) to transport essential ions from the surrounding water into the developing embryo (Hwang & Chou, 2013). As the fish continues to develop, ionocytes migrate to the developing gills and the number of epidermal ionocytes decreases. After all ionocytes have migrated to the gills, the number of ionocytes ceases to increase (Ayson et al., 1994; Hiroi et al., 1999). Gill-localized ionocytes provide adequate respiratory and osmoregulatory capacity in order to meet physiological demands of the organism (Rombough, 2007). When the epidermis is injured, the basal cell layer promotes active cell migration, while the superficial layer utilizes a purse-string contraction to seal off the

wound (Gault et al., 2014). If epidermal cells are damaged, surrounding fluid can disrupt the ion gradients, leading to osmotic and electrical changes within the epidermis such as osmotic shock (Kennard & Theriot, 2020). Osmotic shock may serve as an early cue for epidermal injury, as osmotic shock causes cell swelling, tissue damage within the embryo, and promotion of cellular migration toward the injury (Chen et al., 2019; Gault et al., 2014).

Prolactin is a freshwater-adapting hormone in zebrafish (Breves et al., 2014) that regulates ions and water levels in vertebrates (McCormick & Bradshaw, 2006). Interestingly, prolactin has varying functions in different vertebrates, ranging from 1) wound healing, seasonal hair growth, and milk production in mammals (Foitzik et al., 2009); 2) increasing open-channel density of sodium channels in adult frog skin (Takada & Kasai, 2003); and 3) altering skin permeability of osmoregulatory surfaces (gills, skin, kidney, intestine, bladder) in teleost fish (Manzon, 2002). Prolactin regulates the amount of Na^+, K^+, and Cl^- in embryonic zebrafish (Shu et al., 2016). If prolactin levels are impacted due to chemical exposure, this has the potential to affect regulation of Na^+, K^+, and Cl^- ion transport that is essential for normal zebrafish development.

Prior studies in our lab have found that triphenyl phosphate (TPHP) – a widely used organophosphate-based flame retardant – blocks cardiac looping during zebrafish development in a concentration-dependent manner, a phenotype that is dependent on pericardial edema formation (Isales et al., 2015; McGee et al., 2013; Mitchell et al., 2018; Reddam et al., 2019; Yozzo et al., 2013). Moreover, D-Mannitol – an osmotic diuretic that increases the osmolarity of the surrounding solution (Papich, 2016) – and fenretinide – a synthetic retinoid that may promote epithelial wound repair (Szymański et al., 2020) – are both able to block TPHP-induced pericardial edema (Mitchell et al., 2018, 2019; Reddam et al., 2019; Wiegand et al., 2022, 2023). D-Mannitol does not impact TPHP uptake in

embryos, demonstrating that mitigation of TPHP-induced pericardial edema is not an artifact of decreased embryonic doses of TPHP in the presence of D-Mannitol (Wiegand et al., 2023). TPHP-induced pericardial edema is also associated with increased epidermal ionocyte and microridge formation on the yolk sac epithelium, phenotypes that are rescued by co-exposing embryos to D-Mannitol (Wiegand et al., 2022, 2023). Finally, TPHP-induced pericardial edema does not occur in exposure solutions of low ionic strength (e.g., reverse osmosis water), with edema formation only occurring in exposure solutions with higher ionic strength (e.g., conditioned water from a recirculating system) (Wiegand et al., 2023). Overall, our studies to date collectively suggest that TPHP-induced pericardial edema within zebrafish embryos may be dependent on epidermal injury and disruption of osmoregulation across the epidermis. However, it's currently unclear whether TPHP-induced pericardial edema is reversible or irreversible within embryonic zebrafish.

Using zebrafish embryos as a model, the primary objectives of this study were to 1) determine if TPHP-induced effects on osmoregulation are driven by direct, TPHP-induced injury to the embryonic epidermis and 2) whether TPHP-induced pericardial edema is reversible or irreversible following cessation of exposure, To accomplish these objectives, we first relied on whole-mount immunohistochemistry and automated image analysis to quantify the abundance of prolactin within embryonic zebrafish under varying exposure conditions. Second, we quantified the abundance of embryonic epidermal cells by utilizing DAPI-based, *in situ* staining and automated image analysis. Third, we utilized scanning electron microscopy to determine whether fenretinide blocks TPHP-altered morphology and/or organization of the yolk sac epithelium. Finally, we exposed embryos to TPHP from 24-72 hpf and, after transferring to clean system water from 72-120 hpf,

determined whether the severity of TPHP-induced pericardial edema was associated with TPHP uptake and depuration.

4.3 Materials and Methods

Animals

Using previously described procedures (Mitchell et al., 2018), wildtype adult (strain 5D) zebrafish were maintained and bred on a recirculating system according to an Institutional Animal Care and Use Committee-approved animal use protocol (#20210027) at the University of California, Riverside.

Chemicals

TPHP (99.5% purity), D-mannitol (>98% purity), and fenretinide (>99.3% purity) were purchased from ChemService, Inc. (West Chester, PA, USA), Bio-Techne Corp. (Minneapolis, MN, USA), and Tocris Bioscience (Bristol, UK), respectively. To prepare stock solutions, TPHP and fenretinide were dissolved in liquid chromatography-grade dimethyl sulfoxide (DMSO) and stored at room temperature in 2-mL glass amber vials with polytetrafluoroethylene-lined caps. To prepare working solutions, stock solutions of TPHP and fenretinide were spiked into particulate-free water from our recirculating system (pH and conductivity of ~7-8 and ~900-1000 µS, respectively), resulting in 0.1% DMSO within all vehicle control, fenretinide, and TPHP treatment solutions. D-mannitol solutions were freshly prepared by dissolving powder into particulate-free water from our recirculating system and then immediately used for exposures.

TPHP Exposures

Immediately after spawning, fertilized eggs were collected and incubated in groups of approximately 50 per 100 X 15 mm polystyrene petri dish until 24 h post-fertilization (hpf) within a light- and temperature-controlled incubator. Working solutions of

vehicle (0.1% DMSO), 250 mM D-mannitol, 2.14 µM fenretinide, 5 µM TPHP, 250 mM D-Mannitol + 5 µM TPHP, or 2.14 µM fenretinide + 5 µM TPHP were prepared as described above. The concentrations of D-mannitol, fenretinide, and TPHP were selected based on our previously published studies (Mitchell et al., 2019; Reddam et al., 2019; Wiegand et al., 2022, 2023). Treatment solutions (10 mL per replicate dish) were added to 100 X 15 mm polystyrene petri dishes, and viable embryos were then transferred to dishes, resulting in 30 initial embryos per dish (three replicate dishes per treatment). Embryos were then exposed under static conditions to each treatment solution from 24 to 72 hpf. All dishes were covered with a lid and incubated under a 14-h:10-h light-dark cycle at 28ºC until 72 hpf. At 72 hpf, embryos were fixed overnight at 4ºC in 4% paraformaldehyde (PFA) in 1X phosphate-buffered saline (PBS), transferred to 1X PBS, and stored at 4ºC for no longer than one month until imaging.

To determine whether TPHP-induced pericardial edema was reversible, working solutions of vehicle (0.1% DMSO) and 5 µM TPHP were prepared as described above. Treatment solutions (10 mL per replicate dish) were added to 100 X 15 mm polystyrene petri dishes, and viable embryos were then transferred to dishes, resulting in 30 initial embryos per dish (three replicate dishes per treatment per timepoint). Embryos were then exposed to vehicle (0.1% DMSO) or 5 µM TPHP from 24 to 72 hpf. All dishes were covered with a lid and incubated under a 14-h:10-h light-dark cycle at 28ºC. At 48 and 72 hpf, a total of 90 vehicle-treated embryos and 90 TPHP-treated embryos per time-point were fixed overnight at 4ºC in 4% PFA in 1X PBS, transferred to 1X PBS, and stored at 4ºC for no longer than one month until imaging. The remaining embryos were transferred from vehicle or TPHP solutions into clean water from our recirculating water system and then incubated under a 14-h:10-h light-dark cycle at 28ºC until 96 or 120 hpf. At 96 and 120

hpf, a total of 90 vehicle-treated embryos and 90 TPHP-treated embryos per time-point were fixed overnight at 4ºC in 4% PFA in 1X PBS, transferred to 1X PBS, and stored at 4ºC for no longer than one month until Imaging. Fixed embryos were then transferred to black 384-well microplates containing 0.17-mm glass-bottom wells (Matrical Bioscience, Spokane, WA, USA), centrifuged for 5 min at 140 rpm, and imaged under transmitted light on our ImageXpress Micro XLS Widefield High-Content Screening System within MetaXpress 6.0.3.1658 (Molecular Devices, Sunnyvale, CA, USA). Body length, pericardial area, and yolk sac area were manually quantified within MetaXpress using images captured under transmitted light.

Whole-Mount Immunohistochemistry and Automated Imaging

Similar to previously described protocols (Yozzo et al., 2013), fixed embryos were labeled with 1:500 dilution of a prolactin-specific monoclonal antibody (INN-hPRL-1) (Life Technologies, Carlsbad, CA, USA) and 1:500 dilution of AlexaFluor 488-conjugated goat anti-mouse IgG1 cross-adsorbed antibody (Thermo Fisher Scientific, Waltham, MA, USA) to quantify the abundance of prolactin. Labeled embryos were transferred to black 384-well microplates containing 0.17-mm glass-bottom wells (Matrical Bioscience, Spokane, WA, USA), centrifuged for 5 min at 140 rpm, and imaged under transmitted light and a FITC filter on our ImageXpress Micro XLS Widefield High-Content Screening System within MetaXpress 6.0.3.1658 (Molecular Devices, Sunnyvale, CA, USA). Body length, pericardial area, and yolk sac area were manually quantified within MetaXpress using images captured under transmitted light, whereas prolactin was automatically quantified with a custom module within MetaXpress using images captured under a FITC filter.

Quantification of the Abundance of Embryonic Epidermal Cells

Vehicle- and TPHP-treated embryos were stained with DAPI to quantify the abundance of cells within the embryonic epidermis. Following exposure from 24-72 hpf, 72-hpf embryos were fixed overnight at 4ºC in 4% PFA in 1X PBS, transferred to 1X PBS, and stored at 4ºC for no longer than one month until imaging. Fixed embryos were then incubated at room temperature for 15 min in DAPI-containing Fluoromount-G mounting medium (Thermo Fisher Scientific, Waltham, MA, USA) that was diluted 1:4 in 1X PBS. The solution was then aspirated and embryos were washed with reverse osmosis (RO) water for 5 min. Embryos were then transferred to black 384-well microplates containing 0.17-mm glass-bottom wells (Matrical Bioscience, Spokane, WA, USA), centrifuged for 5 min at 140 rpm, and imaged under transmitted light and a DAPI filter on our ImageXpress Micro XLS Widefield High-Content Screening System within MetaXpress 6.0.3.1658 (Molecular Devices, Sunnyvale, CA, USA). The total area and number of DAPI-labeled epidermal cells were automatically quantified with a custom module within MetaXpress using images captured under a FITC filter.

Quantification of Embryonic Doses of TPHP and DPHP

Embryonic doses of TPHP and diphenyl phosphate (DPHP, the primary metabolite of TPHP) were quantified at 48 hpf, 72 hpf, 96 hpf, and 120 hpf following exposure to vehicle (0.1% DMSO) or 5 μM TPHP from 24-72 hpf and following transfer to clean water from 72-120 hpf as described above. For each replicate (4 replicates per treatment per timepoint), ~30 embryos were placed into a 2-mL cryovial, immediately snap-frozen in liquid nitrogen, and stored at -80°C. Prior to extraction, samples were spiked with deuterated TPHP (d15-TPHP) and deuterated DPHP (d10-DPHP).

Analytes were extracted and quantified according to previously published methods (Mitchell et al., 2018). Method detection limits (MDLs) were set as three times the standard deviation of lab blanks (if present) or three times the noise. The MDLs for TPHP and DPHP were 0.05 ng and 0.45 ng, respectively.

Scanning Electron Microscopy

A Hitachi Tabletop TM4000Plus Scanning Electron Microscope (SEM) was utilized to scan five independent locations on the yolk sac epithelium of each embryo. Prior to imaging, embryos were exposed from 24-72 hpf within RO water, system water, or 2X embryo media (EM) (Wiegand et al., 2023) containing 0.1% DMSO, 5 μM TPHP, 2.14 μM fenretinide, or 5 μM TPHP + 2.14 μM fenretinide as described above. At 72 hpf, all embryos were fixed with 4% PFA and stored as described above. Immediately before imaging, fixed embryos were flash-frozen within a liquid nitrogen bath. Frozen embryos were then imaged using the following magnification and settings: 10 KV, setting 4, VSE, 2,000 X. Images were then analyzed within ImageJ (Version 1.8.0_172) using previously described protocols (Wiegand et al., 2023).

Statistics

For all data generated within this study, a general linear model (GLM) analysis of variance (ANOVA) (α = 0.05) and Tukey-based multiple comparisons were performed within SPSS Statistics 24.

4.4 Results

Ionic Strength of Exposure Media is Associated with Elevated Levels of Prolactin

Relative to embryos exposed to vehicle (0.1% DMSO) from 24-72 hpf, exposure to 5 μM TPHP alone from 24-72 hpf across all three exposure media types (RO Water, System Water, or 2X EM) did not result in a significant increase in prolactin abundance

(Figure 4.1). However, there was an upward trend in prolactin abundance as the ionic strength of exposure media increased from RO Water to System Water to 2X EM, while D-Mannitol alone and TPHP + D-Mannitol co-exposures suppressed prolactin levels across all exposure media types. Pericardial area, yolk sac area, and length across all treatments were consistent with our prior studies (Isales et al., 2015; McGee et al., 2013; Mitchell et al., 2018; Reddam et al., 2019; Wiegand et al., 2022, 2023), where yolk sac area was not affected across treatments nor embryo media types and TPHP induced pericardial edema within embryos exposed within System Water and 2X EM (Figure 4.1).

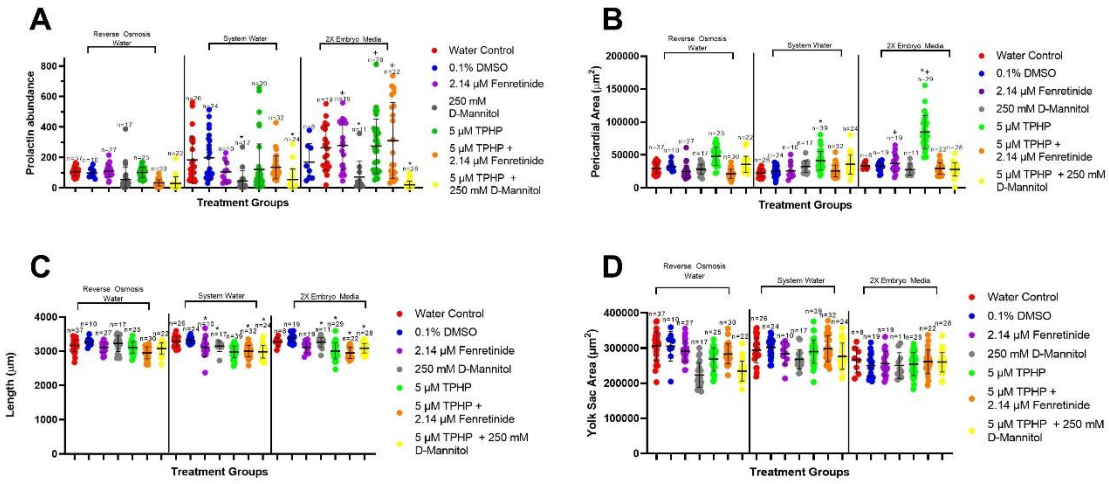

Figure 4.1. Mean (± standard deviation) prolactin fluorescence area (A), pericardial area (B), body length (C), and yolk sac area (D) of embryos exposed to water only, vehicle (0.1% DMSO), 2.14 µM Fenretinide, 250 mM D-Mannitol, 5 µM TPHP, 5 µM TPHP + 2.14 µM Fenretinide, or 5 µM TPHP + 250 mM D-Mannitol from 24-72 hpf. Plus sign (+) denotes a significant difference ($p<0.05$) relative to the same treatment in RO water, whereas asterisk (*) denotes a significant difference ($p<0.05$) relative to embryos exposed to vehicle (0.1% DMSO) within the same media group (RO Water, System Water or 2X EM).

TPHP Does not Decrease DAPI-Positive Cells Within the Embryonic Epidermis

To determine if TPHP has the potential to decrease the number of epidermal cells, embryos were fixed and stained with DAPI following exposure to vehicle (0.1% DMSO), 2.14 µM Fenretinide, 250 mM D-Mannitol, 5 µM TPHP, 5 µM TPHP + 2.14 µM Fenretinide,

or 5 μM TPHP + 250 mM D-Mannitol from 24-72 hpf. Embryos were then analyzed utilizing a custom module within MetaXpress to quantify individual cell nuclei and total area of all nuclei present within the embryonic epidermis. These data were then divided by body length to normalize against embryo size. In RO Water and 2X EM, there were no significant differences in length-normalized total area of nuclei across all treatments. However, in System Water, 2.14 μM Fenretinide, 5 μM TPHP + 2.14 μM Fenretinide, and 5 μM TPHP + 250 mM D-Mannitol resulted in an increase in length-normalized total area of nuclei (Figure 4.2). Interestingly, there was only one treatment – 250 mM D-Mannitol in RO water – that resulted in a significant increase in length-normalized total cell count (Figure 4.2). Body length data were consistent with our prior studies (Isales et al., 2015; McGee et al., 2013; Mitchell et al., 2018, 2019; Reddam et al., 2019; Wiegand et al., 2022, 2023), where exposure to 250 mM D-Mannitol, 5 μM TPHP + 2.14 μM Fenretinide, and 5 μM TPHP + 250 mM D-Mannitol in RO Water resulted in decreased body length when compared to vehicle controls. Similarly, in System Water, exposure to 5 μM TPHP, 5 μM TPHP + 2.14 μM Fenretinide, or 5 μM TPHP + 250 mM D-Mannitol also resulted in decreased body length when compared to vehicle controls. In 2X EM, exposure to 250 mM D-Mannitol, 5 μM TPHP, 5 μM TPHP + 2.14 μM Fenretinide, or 5 μM TPHP + 250 mM D-Mannitol resulted in decreased body length when compared to vehicle controls.

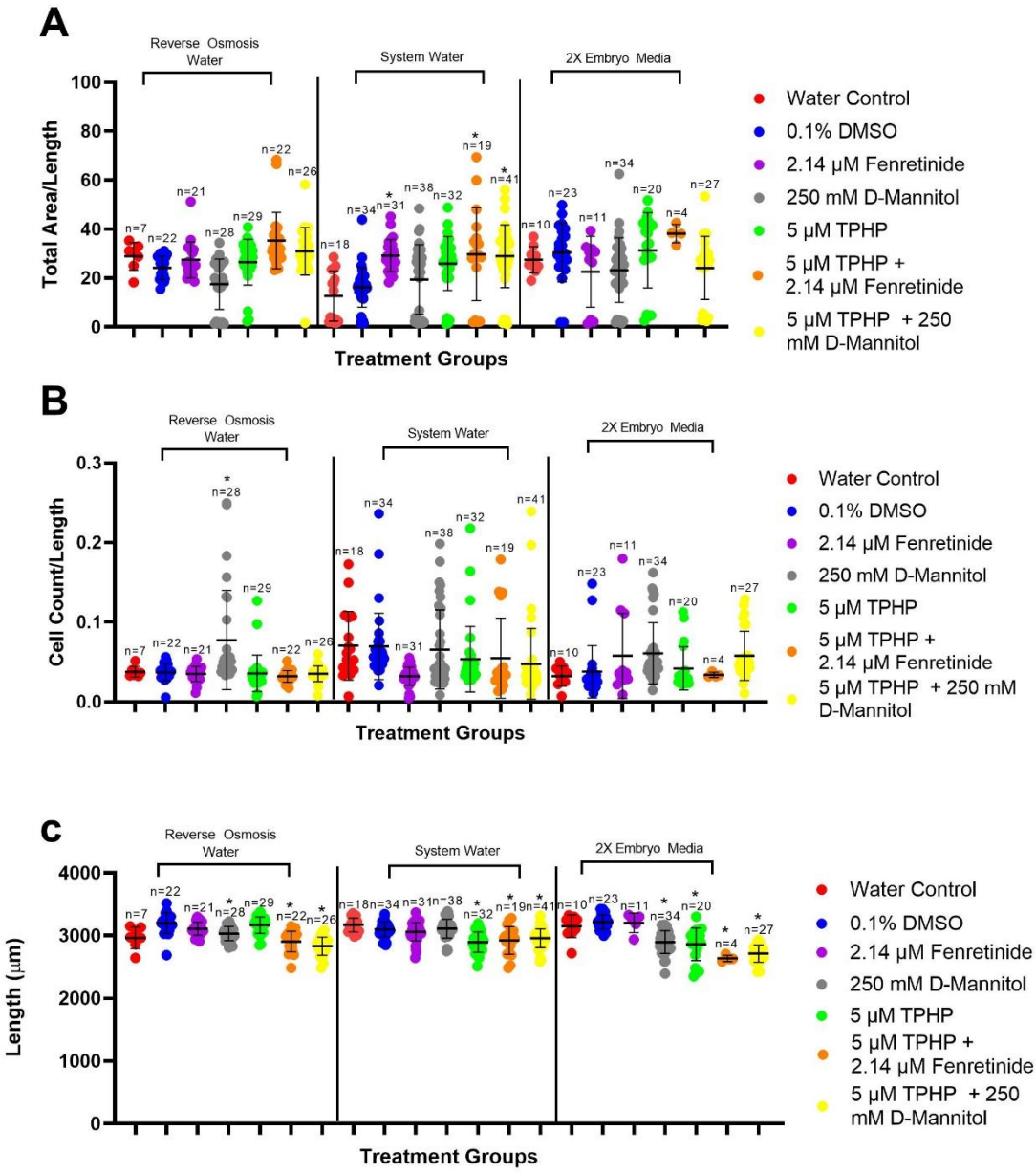

Figure 4.2. Mean (± standard deviation) nuclei area (A) and cell count (B) normalized to the body length (C) of embryos exposed to water only, vehicle (0.1% DMSO), 2.14 μM Fenretinide, 250 mM D-Mannitol, 5 μM TPHP, 5 μM TPHP + 2.14 μM Fenretinide, or 5 μM TPHP + 250 mM D-Mannitol from 24-72 hpf. Plus sign (+) denotes a significant difference ($p<0.05$) relative to the same treatment in RO Water, whereas asterisk (*) denotes a significant difference ($p<0.05$) relative to embryos exposed to vehicle (0.1% DMSO) within the same exposure media (RO Water, System Water or 2X EM).

Fenretinide Mitigates the Prevalence of TPHP-Induced Microridges

Within all SEM imaging locations and exposure media types, 5 μM TPHP induced an increase in the prevalence of microridges on the yolk sac epithelium relative to vehicle controls, with significant differences appearing in 1) Locations A and B in all three exposure types, 2) Location C in System Water and 2X EM, and 3) Locations D and E in 2X EM (Figure 4.3). Embryos exposed to TPHP within 2X EM also exhibited extensive microridges relative to TPHP-exposed embryos in RO Water at Locations A, B and C (Figure 4.6). Interestingly, across all locations, fenretinide partially mitigated the prevalence of TPHP-induced of microridges (Figure 4.6). Consistent with our prior studies (Wiegand et al., 2023), there was an upward trend in the abundance of microridges as a function of increasing ionic strength of exposure media from RO Water to System Water to 2X EM, suggesting that an increase in ionic strength of exposure media alone exacerbates the formation of microridges within the yolk sac epithelium.

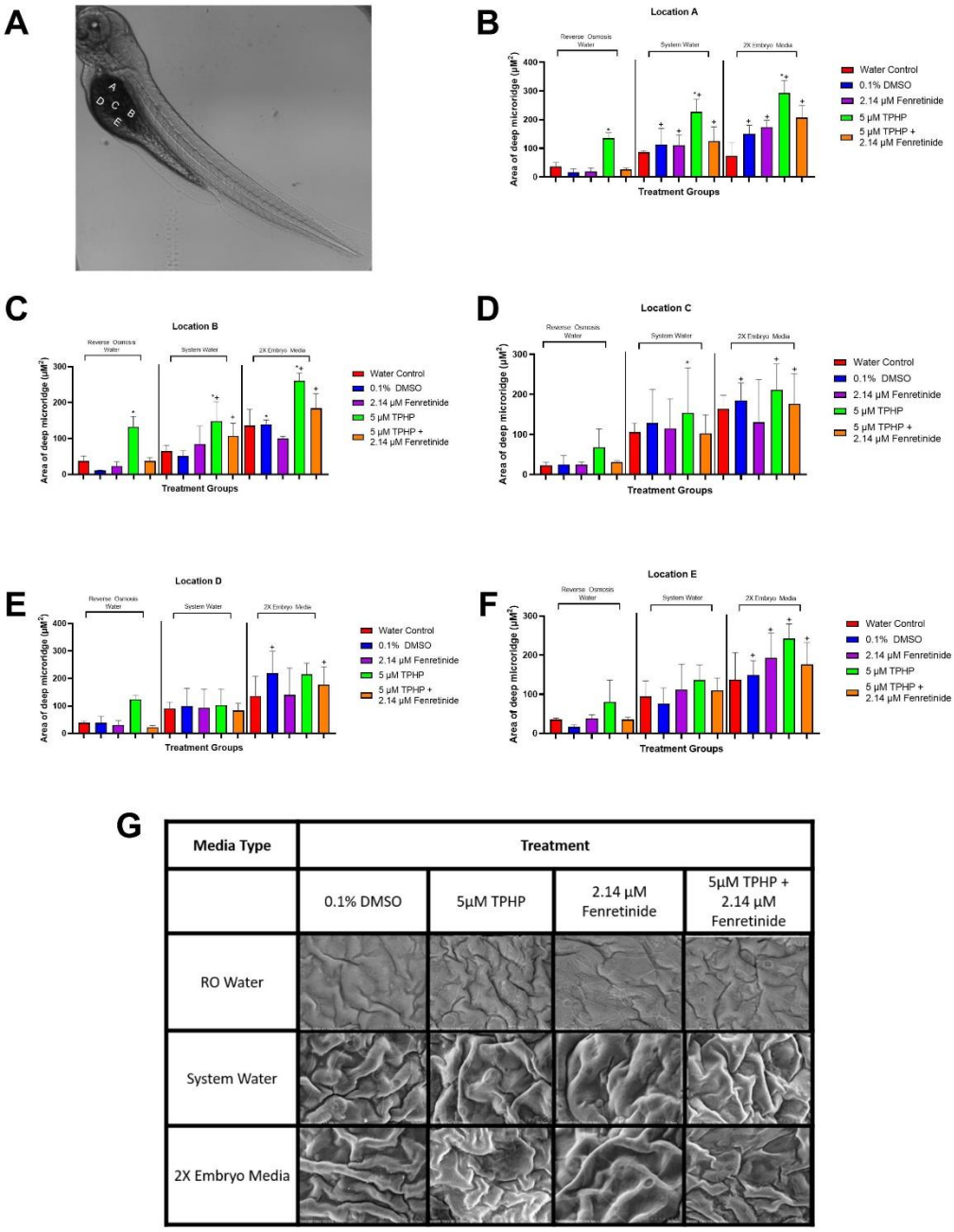

Figure 4.3. Locations (A, B, C, D, and E) used for SEM on the yolk sac epithelium of embryonic zebrafish (A). Panels B-F show the total area of microridges across treatment groups within each location. Representative images of Location C are shown in Panel G. Asterisk (*) denotes a significant difference ($p<0.05$) relative to vehicle (0.1% DMSO) within same exposure medium. Plus sign (+) denotes a significant difference ($p<0.05$) relative to 5 µM TPHP in Reverse Osmosis (RO) Water.

TPHP-Induced Effects on Pericardial Area and Body Length are Reversible

To determine if embryos depurated TPHP after rapid uptake from 24-72 hpf, embryonic doses of TPHP and DPHP were quantified at 48 hpf, 72 hpf, 96 hpf, and 120 hpf. Embryonic doses of TPHP and DPHP were significantly decreased at 96 hpf and 120 hpf after embryos were transferred to clean System Water at 72 hpf (Figure 4.4). Likewise, the severity of TPHP-induced effects on pericardial area and body length was decreased following transfer to clean System Water at 72 hpf, returning to levels similar to vehicle controls by 120 hpf (Figure 4.5).

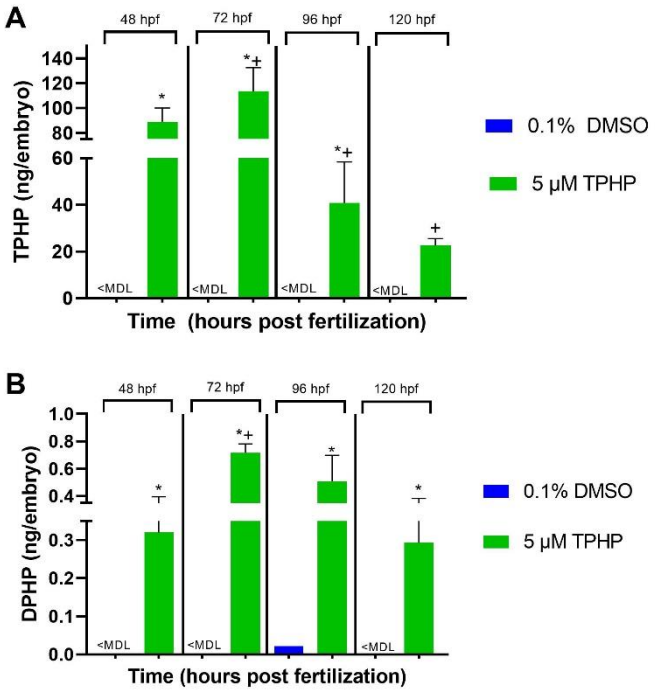

Figure 4.4. Mean (± standard deviation) concentration of TPHP (ng/embryo) (A) and DPHP (ng/embryo) (B) in embryos exposed to vehicle (0.1% DMSO) or 5 µM TPHP from 24-72 hpf. Embryonic doses of TPHP and DPHP were quantified at 48 hpf, 72 hpf, 96 hpf, and 120 hpf. Asterisk (*) denotes a significant difference ($p<0.05$) relative to vehicle (0.1% DMSO) within the same time-point, whereas plus sign (+) denotes a significant difference ($p<0.05$) relative to the same treatment at 48 hpf.

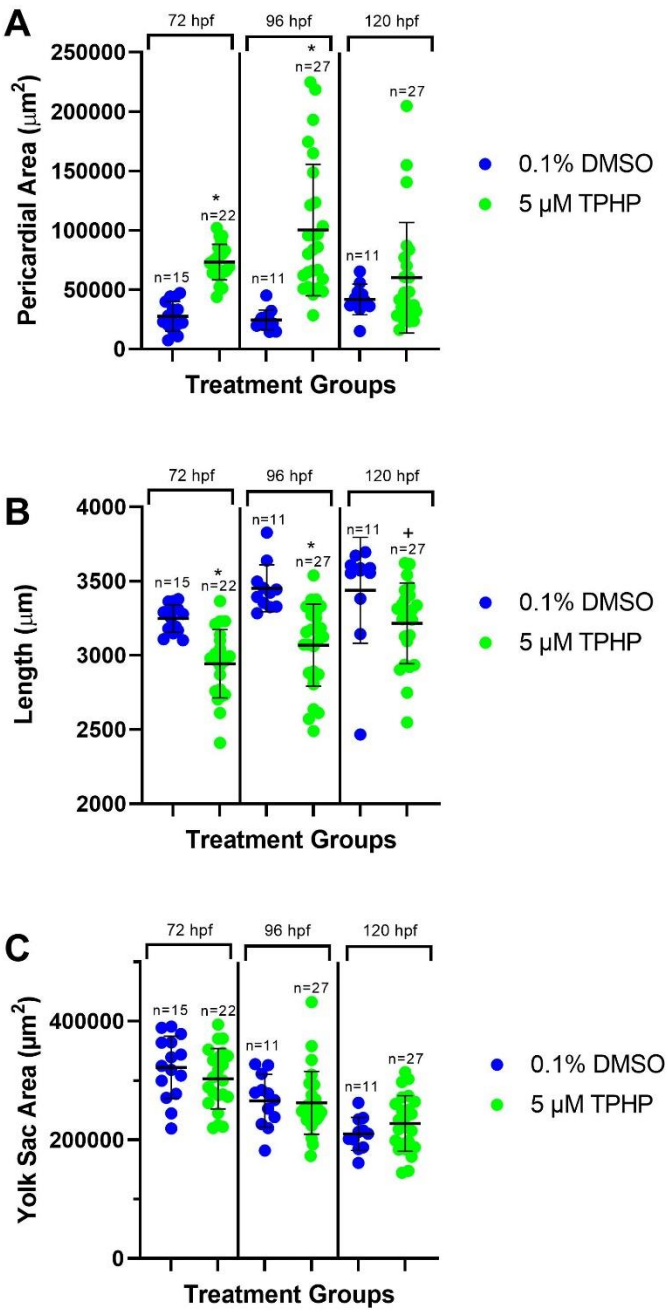

Figure 4.5. Mean (± standard deviation) pericardial area (A), body length (B), and yolk sac area (C) of embryos exposed to vehicle (0.1% DMSO) or 5 μM TPHP from 24-72 hpf and then clean System Water from 72-120 hpf. Asterisk (*) denotes a significant difference ($p<0.05$) relative to vehicle (0.1% DMSO) within the same time-point, whereas plus sign (+) denotes a significant difference ($p<0.05$) relative to the same treatment at 48 hpf.

4.5 Discussion

Based on our prior studies in embryonic zebrafish, we found that TPHP disrupted cardiac looping, induced pericardial edema and liver enlargement, increased ionocyte abundance, and decreased body length (Isales et al., 2015; McGee et al., 2013; Mitchell et al., 2018; Reddam et al., 2019; Wiegand et al., 2022, 2023). In our most recent study, we also found that TPHP-induced pericardial edema was dependent on the ionic strength of exposure media (Wiegand et al., 2023). Although ion-deficient conditions increases prolactin receptor a (*prlra*) in adult zebrafish (Breves et al., 2013), within this study we found that the levels of prolactin in embryonic zebrafish were impacted by the ionic strength of exposure media and not TPHP exposure. Interestingly, prolactin is essential for zebrafish larvae to survive in freshwater, as it allows larval fish to adapt to varying ion levels in the surrounding water (Shu et al., 2016). Moreover, prolactin is a freshwater adaptation hormone (Breves et al., 2014; Manzon, 2002) that is necessary for regulation of the expression of specific ionocytes in zebrafish gills and skin throughout development (Breves et al., 2013, 2014). Therefore, our data suggests that an increase in prolactin as a function of increasing ionic strength of exposure media may be a compensatory response to maintain homeostasis within embryonic zebrafish.

Despite TPHP-induced changes on the yolk sac epithelium (Figure 4.3; Wiegand et al., 2022), TPHP did not decrease DAPI-positive cells within the embryonic epidermis. Prior studies that have investigated embryonic zebrafish skin damage focus on the skin healing process, utilizing methods such as the tail wounding assay, immunohistochemistry, and transgenic lines (LeBert & Huttenlocher, 2014; Richardson, 2018; Rosowski, 2020). Only one study has investigated the impacts of contaminants on the epidermis by utilized a neutral red dye to stain damaged cells (Peng et al., 2018).

DAPI-stained embryos revealed that TPHP did not increase cell death on the epidermis. Although DAPI is a vital dye that identifies live vs. dead cells, DAPI does not reveal non-lethal damage or if junctions between the epidermal cells are being impacted by TPHP. Therefore, it is possible that, in the absence of epidermal cell death, TPHP may induce osmotic shock within the embryonic epidermis due to skin or junction damage, as osmotic shock may alter the ability for embryos to properly regulate ion uptake. Our past study found that that number of ionocytes increase following exposure to TPHP (Wiegand et al., 2022), a compensatory response that might be occurring as a result of trying to regulate an increase in ion concentrations within the embryo.

Based on our most recent study, TPHP exposure resulted in an increase in microridges on the yolk sac epithelium in embryonic zebrafish, and D-Mannitol (an osmoprotectant) was found to block this increase in microridges (Wiegand et al., 2023). Fenretinide – a synthetic retinoid and pan-retinoic acid receptor agonist – was also previously found to reverse pericardial edema within TPHP-exposed embryos (Mitchell et al., 2018). Therefore, similar to D-Mannitol, we hypothesized that fenretinide may block a TPHP-induced increase in microridges on the yolk sac epithelium. Contrary to our hypothesis, fenretinide did not block an increase in TPHP-induced microridges, suggesting that fenretinide-mediated mitigation of TPHP-induced pericardial edema is independent – and possibly downstream – of TPHP-induced microridge formation within the yolk sac epithelium. Although little is known about how contaminants induce the formation of microridges within embryonic zebrafish, it is possible that, given the role of the yolk sac epithelium in osmoregulation, chemically-induced alterations in microridges may impact normal osmoregulation within the embryo (Breves et al., 2014; Dymowska et

al., 2012; Evans, 2008, 2011; Gilmour, 2012; Hiroi & McCormick, 2012; Hwang & Lee, 2007; Hwang et al., 2011; Kumai & Perry, 2012; Wright & Wood, 2012).

Our prior studies also showed that TPHP-induced pericardial edema occurs when embryos are exposed to 5 μM TPHP from 24-72 hpf (Isales et al., 2015; McGee et al., 2013; Mitchell et al., 2018; Reddam et al., 2019; Wiegand et al., 2022, 2023). To determine if TPHP-induced pericardial edema and decreased body length are reversible phenotypes during embryonic development, TPHP-exposed embryos were placed in clean (TPHP-free) system water from 72-120 hpf after being exposed to TPHP from 24-72 hpf. Interestingly, we found that, following transfer to clean water, TPHP-induced pericardial edema was significantly mitigated by 96 and 120 hpf in a time-dependent manner – a finding that was strongly associated with time-dependent depuration from 72-120 hpf. Moreover, there was an approximately 24-h lag between TPHP depuration vs. recovery of embryo morphology based on pericardial area and body length as endpoints, suggesting that TPHP-induced developmental toxicity may be reversible.

4.6 Conclusions

To our knowledge, this is the first study to investigate role of epidermal injury and uptake/depuration kinetics in TPHP-induced pericardial edema within zebrafish embryos. First, we found that exposure to TPHP from 24-72 h post-fertilization (hp) did not increase prolactin in embryonic zebrafish, whereas high ionic strength exposure media was associated with elevated levels of prolactin. Second, we found that TPHP did not decrease DAPI-positive epidermal cells within the embryonic epithelium, and that fenretinide partially mitigated the prevalence of TPHP-induced microridges within the yolk sac epithelium. Finally, we found that the pericardial area of TPHP-exposed embryos was similar to vehicle-treated embryos following transfer to clean water and depuration of

TPHP. Overall, our findings suggest that 1) TPHP does not cause injury to the embryonic epidermis; 2) TPHP-induced pericardial edema is reversible; and 3) the ionic strength of exposure media has the potential to influence the baseline physiology of zebrafish embryos.

Chapter 5: Summary and Conclusions

5.1 Summary

Triphenyl phosphate (TPHP) is a commonly used plasticizer and additive flame retardant that can easily migrate into the environment. Past studies in our lab have shown that TPHP disrupted cardiac looping, induced pericardial edema and liver enlargement, increased ionocyte abundance, and decreased body length in embryonic zebrafish. In Chapter 2, we found that TPHP may have multiple mechanisms of toxicity which leads to an increase in ionocyte abundance and pericardial edema in developing zebrafish embryos. In Chapter 3, we demonstrated that TPHP alters the structure of the yolk sac epithelium, which leads to the disruption of osmoregulation and pericardial edema in zebrafish embryos. Finally, in Chapter 4, our findings suggest that TPHP does not cause injury to the embryonic epidermis, TPHP-induced pericardial edema is reversible and the ionic strength of exposure media has the potential to influence the baseline physiology of zebrafish embryos. Overall, these data highlight the impacts of TPHP on the osmoregulatory system of embryonic zebrafish, and the importance of standardization within the zebrafish toxicology field.

5.2 Triphenyl Phosphate Impacts Ionocyte Abundance

TPHP has been found to block cardiac looping during development which is dependent on TPHP-induced fluid accumulation, increase ionocyte abundance, cause liver enlargement, thyroid endocrine disruption, and ocular toxicity in embryonic zebrafish. Despite our understanding of osmoregulation and the role of ionocytes in embryonic zebrafish, little is known about how environmental contaminants may impact the function and abundance of ionocytes within the embryo. Using immunohistochemistry, we found that TPHP exposure from 24-72 hpf increases the abundance of the Na^+/K^+ ionocytes when compared to the vehicle control. However, D-Mannitol was able to mitigate the

increase in ionocyte abundance as well as pericardial edema formation, which is consistent with past studies. Interestingly, when exposure initiation was changed to 30 hpf, the increase in ionocyte abundance did not occur, but pericardial edema was still present, suggesting that 1) 24-30 hpf represents a critical window of exposure for TPHP-induced effects on ionocyte abundance and 2) an increase in ionocyte abundance may not be required for pericardial edema formation.

To understand if an individual type of Na^+/K^+ ionocyte was required for TPHP-induced pericardial edema to form, a knockdown of ATPase1a1.4 was performed. ATPase1a1.4 was chosen for knockdown because it's strongly expressed and colocalized with NaRCs within the embryonic skin of zebrafish, the alpha subunit contains ion binding sites, and it predominates in freshwater fish. This knockdown mitigated TPHP-induced effects on ionocyte abundance, but not body length or pericardial edema. This suggests that the presence of ATPase1a1.4 is required for TPHP-induced effects on ionocyte abundance.

Finally, to determine whether the absence of functional Na^+/K^+ ionocytes would impact TPHP-induced pericardial edema formation, Ouabain, a broad-spectrum Na^+/K^+ -ATPase inhibitor, was utilized. Interestingly, Ouabain did not increase ionocyte abundance, but it exacerbated the impacts on pericardial area caused by TPHP, suggesting that inhibition of Na^+/K^+-ATPase exacerbates TPHP-induced edema formation. Contrary to D-Mannitol, Ouabain likely facilitated movement from outside to inside the embryo when co-exposed with TPHP. Further research is needed to determine if TPHP is impacting other types of ionocytes, causing an imbalance in ion transport during development and the mechanism of how this is occurring.

5.3 Triphenyl Phosphate-Induced Pericardial Edema is Dependent on the Ionic Strength of Exposure Media

Pericardial edema is the fluid accumulation surrounding the developing heart, it is an abnormal phenotype that has been commonly observed across different species of fish embryos, following exposure to a variety of diverse chemicals. Pericardial edema, depending on severity, can lead to interference in development benchmarks, such as prevention of cardiac looping, bradycardia, and kidney malformations. Past studies have found that in zebrafish embryos, edema may be caused by kidney failure, circulatory failure, ionic imbalance, and permeability defects. While mechanisms underlying edema in mammals has been extensively studied, within the published literature specific to fish, edema is reported as an abnormal phenotype/endpoint, without a follow-up mechanistic investigation. It is possible that edema is being caused by osmoregulatory changes caused by contaminants.

We utilized a fluorescent sodium indicator dye to determine how sodium movement may be impacted by TPHP exposure. Our study found that TPHP does not affect embryonic sodium concentrations *in situ.* To better understand the role of water-borne ions in driving TPHP's impact on embryonic development, ion chromatography and ICP-OES were used to measure the ionic strength of each water type (RO Water, System Water, 0.5X EM, 1X EM, and 2X EM) to better characterize the ionic composition of the exposure media to be used in this study. Fluoride, chloride, nitrite, bromide, nitrate, phosphate, sulfate, sodium, calcium, potassium, and magnesium were measured in five different water samples (RO Water, System Water, 0.5X EM, 1X, EM, 2X EM). Chloride was found to be 3 times higher than the next highest ion (sodium). Utilizing this information, sodium levels were analyzed after TPHP exposures were performed in varying media types. While embryonic sodium concentrations were not affected, TPHP-

induced pericardial edema was. While we found that TPHP decreased body length in all exposure media types, which is consistent with our lab's past studies, pericardial edema did not form in the presence of TPHP in RO Water or 0.5X EM. TPHP-induced pericardial edema did not form until the 1X EM media group. The 2X EM group's edema was so large that it was significantly different from both the vehicle in 2X EM and the TPHP exposed embryos in the RO group. This suggests that high ionic strength in exposure media is required for TPHP-induced pericardial edema formation. Each ingredient of the embryo media was then tested to determine if there was a particular ion which was contributing to the edema formation. While there were no significant differences in body length of yolk sac area across all groups, pericardial area was significantly increased when embryos were exposed to TPHP within exposure media containing any of the four EM ingredients. Interestingly the most significant effects were observed when embryos were exposed within exposure media containing KCl, $CaCl_2 \bullet 2H_2O$, or NaCl, suggesting that chloride may be playing a key role in pericardial edema formation.

Analytical chemistry was performed to ensure that changes in ionic strength were not impacting TPHP uptake and preventing edema formation. Analytical chemistry was also performed on embryos exposed to TPHP and D-Mannitol, as D-Mannitol has been found to block edema formation from occurring in embryonic zebrafish. It was found that ionic strength of exposure media and D-Mannitol do not impact uptake of TPHP into the embryos, indicating that another mechanism is causing the differences in edema formation.

In our past study, we found that TPHP impacts the abundance of Na^+/K^+ ionocytes. Given that ionocytes are found alongside the skin of embryonic zebrafish until 14 dpf, with a large amount of them being found in the yolk sac, looking at the epithelial layer of the yolk sac may elucidate a mechanism of toxicity for TPHP. A scanning electron microscope

was used to analyze if TPHP induced alterations to the yolk sac epithelium, and TPHP disrupts the morphology and organization of the embryonic yolk sac epithelium by increasing the abundance of microridges. While microridges in TPHP-exposed embryos were higher at all locations, we only observed significant differences in two of the study locations. Interestingly, embryos that were exposed to TPHP and D-Mannitol had significantly less microridges compared to embryos exposed to TPHP alone. At all locations analyzed, there is an upward trend in the abundance of microridges observed within TPHP-exposed embryos. This suggests that an increase in ionic strength of exposure media exacerbated the generation of microridges within embryos.

5.4 TPHP-Induced Pericardial Edema is Reversible

Chapters 2 and 3 found that osmoregulation and yolk sac epithelium morphology/organization are being impacted in embryonic zebrafish that are exposed to TPHP. Our lab has also previously found that pre-treatment and/or co-exposure with fenretinide (a synthetic retinoid and pan-retinoic acid receptor agonist) or D-Mannitol (an osmoprotectant) blocks pericardial edema formation in embryos that are exposed to TPHP. Both drugs have different structures and mechanisms of action, but D-Mannitol and Fenretinide can block or mitigate key events that lead to pericardial edema formation. To determine how this is occurring, we identified how TPHP is impacting prolactin (a critical hormone that plays a role in wound healing and osmoregulation), extended exposure durations from 24-72 hpf to 24-120 hpf, and utilized a DAPI stain to quantify the DAPI-positive cells on embryonic zebrafish's epithelial layer.

Immunohistochemistry was performed to determine prolactin abundance in embryos, and while TPHP does not seem to impact prolactin abundance, the ionic strength of the exposure media seems to be associated with elevated levels of prolactin. Interestingly, prolactin is essential for zebrafish larvae to survive in freshwater, and is

considered a freshwater adaption hormone, that is necessary for regulation of the expression of specific ionocytes through zebrafish development. Our data suggests that the increase seen in prolactin may be a compensatory response to maintain homeostasis in embryonic zebrafish.

To determine in TPHP exposure can cause a decrease in the number of epidermal cells, a DAPI stain was used. We found that TPHP does not decrease DAPI-positive cells within the embryonic epidermis. However, in System Water, 2.14 μM Fenretinide, 5 μM TPHP + 2.14 μM Fenretinide, and 5 μM TPHP + 250 mM D-Mannitol resulted in an increase in length-normalized total area of nuclei. Interestingly, there was only one treatment – 250 mM D-Mannitol in RO water – that resulted in a significant increase in length-normalized total cell count.

Based on Chapter 3, TPHP exposure resulted in an increase in microridge abundance on the yolk sac epithelium in embryonic zebrafish, which D-Mannitol was able to block this phenotype. To determine if fenretinide (which can also reverse pericardial edema within TPHP-exposed embryos) blocks TPHP-induced microridge formation, scanning electron microscopy was performed. Interestingly, fenretinide did not block the increase in TPHP-induced microridges, suggesting that fenretinide-meditated mitigation of TPHP-induced pericardial edema is independent of TPHP-induced microridge formation.

To determine if embryos were able to depurate TPHP after uptake from 24-72 hpf, embryonic doses of TPHP and DPHP were quantified at 48 hpf, 72 hpf, 96 hpf, and 120 hpf. TPHP exposures were performed from 24-72 and then embryos were placed in clean system water from 72-120 hpf. Body length, yolk sac edema and pericardial area were quantified at 72, 96 hpf and 120 hpf. Embryonic doses of TPHP and DPHP were significantly decreased at 96 hpf and 120 hpf after transfer to clean System Water. Also,

TPHP-induced effects on pericardial area and body length are reversible and returned to levels similar to vehicle controls by 120 hpf.

5.5 Further Directions and Considerations

Edema is a commonly observed abnormal phenotype in fish toxicological studies. Despite its widespread use, the mechanism of edema formation is unknown. Therefore, determining this mechanism of action, and whether it is consistent throughout edema causing contaminants is essential. The research conducted within Chapter 2, Chapter 3 and Chapter 4 utilized zebrafish embryos, an animal model commonly used to assess the effects of contaminants during development. Due to its rapid development, overlap with other vertebrate development processes, small size, and fully sequenced genome, the zebrafish is an ideal model to perform toxicity testing. Commonly used experimental methods were also utilized to analyze TPHP toxicity and to determine the edema-causing mechanism. The research presented within this dissertation has aimed to fill some of the gaps associated with TPHP-induced impacts on development, as well as the mechanisms that cause edema to form in embryonic zebrafish. Our research addresses 1) the impacts of TPHP on the osmoregulatory system of zebrafish embryos, 2) the impact of an exposure media's ionic strength on edema formation in embryonic zebrafish, 3) how TPHP impacts the epithelial layer of embryonic zebrafish.

Despite the novel nature of this dissertation, it has provided a wide variety of questions that still need to be answered. For example, we predict that the increase in ionocytes seen in Chapter 2, likely plays a role in edema formation, yet our understanding of where this falls in TPHP's adverse outcome pathway is limited. We can predict that it falls later in our adverse outcome pathway, likely before fluid accumulation occurs (Figure 5.1), though our work never confirmed this. Our work has also not been able to identify

the initiating action of pericardial edema formation. Future work should continue to look at various factors that could play a role in the adverse outcome pathway. Future studies could include looking at TPHP's impact on tight junctions between the keratinocytes on the embryo's epithelium utilizing whole-mount immunohistochemistry or morpholino knockdowns. Other studies could include looking at other hormones that regulate osmotic and ionic homeostasis such as, cortisol, isotocin-neurophysin, atrial natriuretic peptide, renin, catecholamines, growth hormone, parathyroid hormone, and calcitonin.

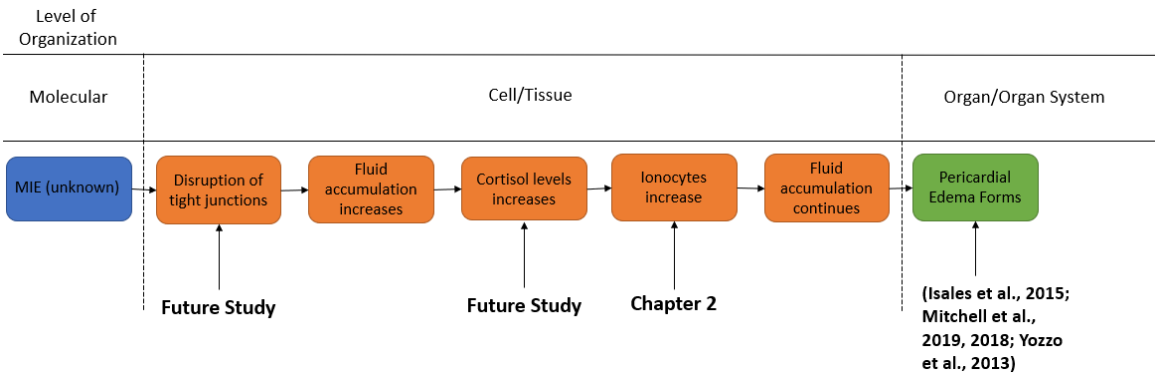

Figure 5.1: The predicted adverse outcome pathway based on past studies as well as Chapters 2-4. It includes two steps that will need to be further experimented on to determine if they play a role in pericardial edema formation.

In Chapter 4, we found that fenretinide, a RAR agonist was able to mitigate pericardial edema, and the increase in microridges on the yolk sac epithelium. Despite this knowledge, little is known about how TPHP is impacting the RAR nuclear receptors in embryonic zebrafish. There is also little information on TPHP's impacts on other nuclear receptors. Looking further into this relationship could also potentially elucidate a mechanism of action for edema formation.

The continuation of this work is essential to determine the validity of zebrafish as a toxicology model, as well as determining the mechanism of edema formation in zebrafish embryos. For example, future studies should focus on analyzing the yolk sac epithelium

at 120 hpf (using SEM) to determine if microridge abundance is reversible like the TPHP-induced pericardial edema and shortened body length. Finally, using zebrafish embryos, the toxicity of a library of edema-inducing chemicals should be screened in varying exposure media as well as in the presence/absence of D-Mannitol to determine whether our findings with TPHP apply to other environmental chemicals or drugs that are known to induce pericardial edema.

References

Antkiewicz, D., Burns, C., Carney, S., Peterson, R., & Heideman, W. (2005). Heart malformation is an early response to TCDD in embryonic zebrafish. *Toxicological Sciences : An Official Journal of the Society of Toxicology*, *84*(2), 368–377. https://doi.org/10.1093/TOXSCI/KFI073

Ayson, F. G., Kaneko, T., Hasegawa, S., & Hirano, T. (1994). Development of mitochondrion-rich cells in the yolk-sac membrane of embryos and larvae of tilapia, Oreochromis mossambicus, in fresh water and seawater. *Journal of Experimental Zoology*, *270*(2), 129–135. https://doi.org/10.1002/JEZ.1402700202

Begemann, G., Marx, M., Mebus, K., Meyer, A., & Bastmeyer, M. (2004). Beyond the neckless phenotype: Influence of reduced retinoic acid signaling on motor neuron development in the zebrafish hindbrain. *Developmental Biology*, *271*(1), 119–129. https://doi.org/10.1016/j.ydbio.2004.03.033

BK, L., RD, C., & PP, H. (2009). Expression regulation of Na+-K+-ATPase alpha1-subunit subtypes in zebrafish gill ionocytes. *American Journal of Physiology. Regulatory, Integrative and Comparative Physiology*, *296*(6). https://doi.org/10.1152/AJPREGU.00029.2009

Breves, J. P., McCormick, S. D., & Karlstrom, R. O. (2014). Prolactin and teleost ionocytes: new insights into cellular and molecular targets of prolactin in vertebrate epithelia. *General and Comparative Endocrinology*, *0*, 21. https://doi.org/10.1016/J.YGCEN.2013.12.014

Breves, J. P., Serizier, S. B., Goffin, V., Mccormick, S. D., & Karlstrom, R. O. (2013). *Prolactin regulates transcription of the ion uptake Na + /Cl − cotransporter (ncc) gene in zebrafish gill*. https://doi.org/10.1016/j.mce.2013.01.021

Breves, J. P., Starling, J. A., Popovski, C. M., Doud, J. M., & Tipsmark, C. K. (2020). Salinity-dependent expression of ncc2 in opercular epithelium and gill of mummichog (Fundulus heteroclitus). *Journal of Comparative Physiology. B, Biochemical, Systemic, and Environmental Physiology*, *190*(2), 219–230. https://doi.org/10.1007/S00360-020-01260-X

Carney, T. J., von der Hardt, S., Sonntag, C., Amsterdam, A., Topczewski, J., Hopkins, N., & Hammerschmidt, M. (2007). Inactivation of serine protease Matriptase1a by its inhibitor Hai1 is required for epithelial integrity of the zebrafish epidermis. *Development (Cambridge, England)*, *134*(19), 3461–3471. https://doi.org/10.1242/DEV.004556

Chang, W. J., & Hwang, P. P. (2011). Development of zebrafish epidermis. *Birth Defects Research. Part C, Embryo Today : Reviews*, *93*(3), 205–214. https://doi.org/10.1002/BDRC.20215

Chen, D., Zhang, J., & Chen, Y. ping. (2021). Ecotoxicity assessment of a molybdenum mining effluent using acute lethal, oxidative stress, and osmoregulatory endpoints in zebrafish (Danio rerio). *Environmental Science and Pollution Research*, *28*(5), 5137–5148. https://doi.org/10.1007/S11356-020-10841-W/TABLES/3

Chen, L. M., Zhao, J., Musa-Aziz, R., Pelletier, M. F., Drummond, I. A., & Boron, W. F. (2010). Cloning and characterization of a zebrafish homologue of human AQP1: A bifunctional water and gas channel. *American Journal of Physiology - Regulatory Integrative and Comparative Physiology*. https://doi.org/10.1152/ajpregu.00319.2010

Chen, T., Zhao, H., Gao, L., Song, L., Yang, F., & Du, J. (2019). Hypotonicity promotes epithelial gap closure by lamellipodial protrusion. *Progress in Biophysics and Molecular Biology*, *148*, 60–64. https://doi.org/10.1016/j.pbiomolbio.2017.09.021

Chen, Y., Ren, C., Ouyang, S., Hu, X., & Zhou, Q. (2015). Mitigation in Multiple Effects of Graphene Oxide Toxicity in Zebrafish Embryogenesis Driven by Humic Acid. *Environmental Science & Technology*, *49*(16), 10147–10154. https://doi.org/10.1021/ACS.EST.5B02220

Cheng, V., Dasgupta, S., Reddam, A., & Volz, D. C. (2019). Ciglitazone-a human PPARã agonist-disrupts dorsoventral patterning in zebrafish. *PeerJ*, *2019*(11), e8054. https://doi.org/10.7717/peerj.8054

Choi, J. H., Lee, K. M., Inokuchi, M., & Kaneko, T. (2011). Morphofunctional modifications in gill mitochondria-rich cells of Mozambique tilapia transferred from freshwater to 70% seawater, detected by dual observations of whole-mount immunocytochemistry and scanning electron microscopy. *Comparative Biochemistry and Physiology. Part A, Molecular & Integrative Physiology*, *158*(1), 132–142. https://doi.org/10.1016/J.CBPA.2010.09.019

Choi, S. A., Park, C. S., Kwon, O. S., Giong, H. K., Lee, J. S., Ha, T. H., & Lee, C. S. (2016). Structural effects of naphthalimide-based fluorescent sensor for hydrogen sulfide and imaging in live zebrafish. *Scientific Reports*, *6*. https://doi.org/10.1038/SREP26203

Chretien, M., & Pisam, M. (1986). Cell renewal and differentiation in the gill epithelium of fresh- or salt-water-adapted euryhaline fish as revealed by [3H]-thymidine radioautography [Lebistes reticulatus]. *Biology of the Cell*, *56*(2), 137–150. https://agris.fao.org/agris-search/search.do?recordID=FR8604846

Cindrova-Davies, T., Jauniaux, E., Elliot, M. G., Gong, S., Burton, G. J., & Charnock-Jones, D. S. (2017). RNA-seq reveals conservation of function among the yolk sacs of human, mouse, and chicken. *Proceedings of the National Academy of Sciences of the United States of America*, *114*(24), E4753–E4761. https://doi.org/10.1073/PNAS.1702560114

Conte, F. P. (2012). Origin and differentiation of ionocytes in gill epithelium of teleost fish. In *International Review of Cell and Molecular Biology*. https://doi.org/10.1016/B978-0-12-394310-1.00001-1

Conte, F. P., & Lin, D. H. Y. (1967). Kinetics of cellular morphogenesis in gill epithelium during sea water adaptation of oncorhynchus (walbaum). *Comparative Biochemistry and Physiology*, *23*(3). https://doi.org/10.1016/0010-406X(67)90355-6

Dasgupta, S., Dunham, C. L., Truong, L., Simonich, M. T., Sullivan, C. M., & Tanguay, R. L. (2021). Phenotypically Anchored mRNA and miRNA Expression Profiling in Zebrafish Reveals Flame Retardant Chemical Toxicity Networks. *Frontiers in Cell and Developmental Biology*, *9*. https://doi.org/10.3389/fcell.2021.663032

Dave, P. H., & Kwong, R. W. M. (2020). Cadmium exposure reduces the density of a specific ionocyte subtype in developing zebrafish. *Chemosphere*, *244*, 125535. https://doi.org/10.1016/j.chemosphere.2019.125535

Dejana, E., Tournier-Lasserve, E., & Weinstein, B. M. (2009). The Control of Vascular Integrity by Endothelial Cell Junctions: Molecular Basis and Pathological Implications. *Developmental Cell*, *16*(2), 209–221. https://doi.org/10.1016/J.DEVCEL.2009.01.004

Dolgova, N. V., Hackett, M. J., MacDonald, T. C., Nehzati, S., James, A. K., Krone, P. H., George, G. N., & Pickering, I. J. (2016). Distribution of selenium in zebrafish larvae after exposure to organic and inorganic selenium forms. *Metallomics : Integrated Biometal Science*, *8*(3), 305–312. https://doi.org/10.1039/C5MT00279F

Du, Z., Zhang, Y., Wang, G., Peng, J., Wang, Z., & Gao, S. (2016). TPhP exposure disturbs carbohydrate metabolism, lipid metabolism, and the DNA damage repair system in zebrafish liver. *Scientific Reports*, *6*(1), 1–10. https://doi.org/10.1038/srep21827

Duan, J., Yu, Y., Shi, H., Tian, L., Guo, C., Huang, P., Zhou, X., Peng, S., & Sun, Z. (2013). Toxic Effects of Silica Nanoparticles on Zebrafish Embryos and Larvae. *PLoS ONE*, *8*(9), e74606. https://doi.org/10.1371/journal.pone.0074606

Dymowska, A. K., Hwang, P. P., & Goss, G. G. (2012). *Structure and function of ionocytes in the freshwater fish gill*. *184*(3), 282–292. https://doi.org/10.1016/J.RESP.2012.08.025

Esaki M, Hoshijima K, Nakamura N, & et al. (2009). Mechanism of Development of Ionocytes Rich in Vacuolar-Type H(+)-ATPase in the Skin of Zebrafish Larvae. *Developmental Biology*, *329*(1), 116–129. https://doi.org/10.1016/j.ydbio.2009.02.026

Esbaugh, A. J., Brix, K. V., & Grosell, M. (2019). Na+ K+ ATPase isoform switching in zebrafish during transition to dilute freshwater habitats. *Proceedings of the Royal Society B*, *286*(1903). https://doi.org/10.1098/RSPB.2019.0630

Evans, D. (2008). Teleost fish osmoregulation: What have we learned since August Krogh, Homer Smith, and Ancel Keys. *American Journal of Physiology - Regulatory Integrative and Comparative Physiology*, *295*(2). https://doi.org/10.1152/AJPREGU.90337.2008/SUPPL_FILE/DESCRIPTIONS.DOCX

Evans, D. (2011). Freshwater Fish Gill Ion Transport: August Krogh to morpholinos and microprobes. *Acta Physiologica*, *202*(3), 349–359. https://doi.org/10.1111/J.1748-1716.2010.02186.X

Evans, D., Piermarini, P. M., & Choe, K. P. (2005). The multifunctional fish gill: dominant site of gas exchange, osmoregulation, acid-base regulation, and excretion of nitrogenous waste. *Physiological Reviews*, *85*(1), 97–177. https://doi.org/10.1152/PHYSREV.00050.2003

Evans, D., Piermarini, P. M., & Potts, W. T. W. (1999). Ionic Transport in the Fish Gill Epithelium. *JOURNAL OF EXPERIMENTAL ZOOLOGY*, *283*, 641–652.

Fan, Q., Zou, X., Gao, J., Cheng, Y., Wang, C., Feng, Z., Ding, Y., & Zhang, C. (2021). Assessing ecological risk of organophosphate esters released from sediment with both of total content and desorbable content. *Science of the Total Environment*, *772*, 144907. https://doi.org/10.1016/j.scitotenv.2020.144907

Foitzik, K., Langan, E. A., & Paus, R. (2009). Prolactin and the Skin: A Dermatological Perspective on an Ancient Pleiotropic Peptide Hormone. *Journal of Investigative Dermatology*, *129*(5), 1071–1087. https://doi.org/10.1038/JID.2008.348

Fridman, S. (2020). Ontogeny of the Osmoregulatory Capacity of Teleosts and the Role of Ionocytes. *Frontiers in Marine Science*. https://doi.org/10.3389/fmars.2020.00709

Gao, L., Shi, Y., Li, W., Liu, J., & Cai, Y. (2016). Occurrence and distribution of organophosphate triesters and diesters in sludge from sewage treatment plants of Beijing, China. *Science of the Total Environment*, *544*, 143–149. https://doi.org/10.1016/j.scitotenv.2015.11.094

Garcia, G. R., Bugel, S. M., Truong, L., Spagnoli, S., & Tanguay, R. L. (2018). AHR2 required for normal behavioral responses and proper development of the skeletal and reproductive systems in zebrafish. *PLOS ONE*, *13*(3), e0193484. https://doi.org/10.1371/JOURNAL.PONE.0193484

Gault, W. J., Enyedi, B., & Niethammer, P. (2014). Osmotic surveillance mediates rapid wound closure through nucleotide release. *Journal of Cell Biology*, *207*(6), 767–782. https://doi.org/10.1083/jcb.201408049

Ge, C., Lu, W., & Chen, A. (2017). Quantitative proteomic reveals the dynamic of protein profile during final oocyte maturation in zebrafish. *Biochemical and Biophysical Research Communications*, *490*(3), 657–663. https://doi.org/10.1016/J.BBRC.2017.06.093

Gilmour, K. M. (2012). New insights into the many functions of carbonic anhydrase in fish gills. *Respiratory Physiology & Neurobiology*, *184*(3), 223–230. https://doi.org/10.1016/J.RESP.2012.06.001

Goodale, B. C., la Du, J. K., Bisson, W. H., Janszen, D. B., Waters, K. M., & Tanguay, R. L. (2012). AHR2 mutant reveals functional diversity of aryl hydrocarbon receptors in zebrafish. *PloS One*, *7*(1). https://doi.org/10.1371/JOURNAL.PONE.0029346

Green, N., Schlabach, M., Bakke, T., Brevik, E., Dye, C., Herzke, D., Huber, S., Plosz, B., Remberger, M., Schøyen, M., Uggerud, H. T., & Vogelsang, C. (2007). SCREENING OF SELECTED METALS AND NEW ORGANIC CONTAMINANTS 2007. In *104*. Norsk institutt for vannforskning. https://niva.brage.unit.no/niva-xmlui/handle/11250/213998

Guh, Y. J., Lin, C. H., & Hwang, P. P. (2015). Osmoregulation in zebrafish: Ion transport mechanisms and functional regulation. *EXCLI Journal*, *14*, 627–659. https://doi.org/10.17179/excli2015-246

Hagedorn, M., Kleinhans, F. W., Artemov, D., & Pilatus, U. (1998). Characterization of a Major Permeability Barrier in the Zebrafish Embryo. *Biology of Reproduction*, *59*(5), 1240–1250. https://doi.org/10.1095/BIOLREPROD59.5.1240

Hermsen, S. A. B., van den Brandhof, E. J., van der Ven, L. T. M., & Piersma, A. H. (2017). Relative embryotoxicity of two classes of chemicals in a modified zebrafish embryotoxicity test and comparison with their in vivo potencies. *Toxicology in Vitro*, *25*(3), 745–753. https://doi.org/10.1016/J.TIV.2011.01.005

Hill, A., Bello, S., Prasch, A., Peterson, R., & Heideman, W. (2004). Water permeability and TCDD-induced edema in zebrafish early-life stages. *Toxicological Sciences : An Official Journal of the Society of Toxicology*, *78*(1), 78–87. https://doi.org/10.1093/TOXSCI/KFH056

Hiroi, J., Kaneko, T., & Tanaka, M. (1999). In vivo sequential changes in chloride cell morphology in the yolk-sac membrane of mozambique tilapia (Oreochromis mossambicus) embryos and larvae during seawater adaptation. *The Journal of Experimental Biology*, *202 Pt 24*(24), 3485–3495. https://doi.org/10.1242/JEB.202.24.3485

Hiroi, J., & McCormick, S. D. (2012). New insights into gill ionocyte and ion transporter function in euryhaline and diadromous fish. *Respiratory Physiology & Neurobiology*, *184*(3), 257–268. https://doi.org/10.1016/J.RESP.2012.07.019

Hirose, S., Kaneko, T., Naito, N., & Takei, Y. (2003). Molecular biology of major components of chloride cells. *Comparative Biochemistry and Physiology - B Biochemistry and Molecular Biology*, *136*(4), 593–620. https://doi.org/10.1016/S1096-4959(03)00287-2

Hong, X., Chen, R., Hou, R., Yuan, L., & Zha, J. (2018). *Triphenyl Phosphate (TPHP)-Induced Neurotoxicity in Adult Male Chinese Rare Minnows (Gobiocypris rarus)*. *52*(20). https://doi.org/10.1021/acs.est.8b04079

Hootman, S. R., & Philpott, C. W. (1980). Accessory cells in teleost branchial epithelium. *The American Journal of Physiology*, *238*(3). https://doi.org/10.1152/AJPREGU.1980.238.3.R199

Hsiao, C. Der, You, M. S., Guh, Y. J., Ma, M., Jiang, Y. J., & Hwang, P. P. (2007). A positive regulatory loop between foxi3a and foxi3b is essential for specification and differentiation of zebrafish epidermal ionocytes. *PLoS ONE*. https://doi.org/10.1371/journal.pone.0000302

Hsu, H. H., Lin, L. Y., Tseng, Y. C., Horng, J. L., & Hwang, P. P. (2014). A new model for fish ion regulation: identification of ionocytes in freshwater- and seawater-acclimated medaka (Oryzias latipes). *Cell and Tissue Research*, *357*(1), 225–243. https://doi.org/10.1007/S00441-014-1883-Z

Hwang, P. -P. (1988). Multicellular complex of chloride cells in the gills of freshwater teleosts. *Journal of Morphology*, *196*(1), 15–22. https://doi.org/10.1002/JMOR.1051960103

Hwang, P, & Lee, T. H. (2007). New insights into fish ion regulation and mitochondrion-rich cells. In *Comparative Biochemistry and Physiology - A Molecular and Integrative Physiology* (Vol. 148, Issue 3, pp. 479–497). Pergamon. https://doi.org/10.1016/j.cbpa.2007.06.416

Hwang, Pung, & Chou, M. Y. (2013). Zebrafish as an animal model to study ion homeostasis. *Pflugers Archiv : European Journal of Physiology*, *465*(9), 1233–1247. https://doi.org/10.1007/S00424-013-1269-1

Hwang, Pung, Lee, T. H., & Lin, L. Y. (2011). Ion regulation in fish gills: Recent progress in the cellular and molecular mechanisms. *American Journal of Physiology - Regulatory Integrative and Comparative Physiology*, *301*(1), 28–47. https://doi.org/10.1152/AJPREGU.00047.2011/ASSET/IMAGES/LARGE/ZH60061175900004.JPEG

Hwang, Pung, & Lin, L.-Y. (2013). *Gill Ionic Transport, Acid-Base Regulation, and Nitrogen Excretion* (D. H. Evans, J. . Claiborne, & S. Currie (eds.); The Physio). CRC Press. https://books.google.com/books?hl=en&lr=&id=KHtcAgAAQBAJ&oi=fnd&pg=PA205&dq=Gill+ionic+transport,+acid-base+regulation,+and+nitrogen+excretion&ots=Q9E5D0as_9&sig=iDabql97zE5letDDlgLbX5cpi9w#v=onepage&q=Gill ionic transport%2C acid-base regulation%2C and n

Inokuchi, M., & Kaneko, T. (2012). Recruitment and degeneration of mitochondrion-rich cells in the gills of Mozambique tilapia Oreochromis mossambicus during adaptation to a hyperosmotic environment. *Comparative Biochemistry and Physiology. Part A, Molecular & Integrative Physiology*, *162*(3), 245–251. https://doi.org/10.1016/J.CBPA.2012.03.018

Inokuchi, M., Nakamura, M., Miyanishi, H., Hiroi, J., & Kaneko, T. (2017). Functional classification of gill ionocytes and spatiotemporal changes in their distribution after transfer from seawater to freshwater in Japanese seabass. *Journal of Experimental Biology*, *220*(24), 4720–4732. https://doi.org/10.1242/jeb.167320

Isales, G. M., Hipszer, R. A., Raftery, T. D., Chen, A., Stapleton, H. M., & Volz, D. C. (2015). Triphenyl phosphate-induced developmental toxicity in zebrafish: Potential role of the retinoic acid receptor. *Aquatic Toxicology*, *161*, 221–230. https://doi.org/10.1016/j.aquatox.2015.02.009

Jänicke, M., Carney, T. J., & Hammerschmidt, M. (2007). Foxi3 transcription factors and Notch signaling control the formation of skin ionocytes from epidermal precursors of the zebrafish embryo. *Developmental Biology*. https://doi.org/10.1016/j.ydbio.2007.04.044

Jarema, K. A., Hunter, D. L., Shaffer, R. M., Behl, M., & Padilla, S. (2015). Acute and developmental behavioral effects of flame retardants and related chemicals in zebrafish. *Neurotoxicology and Teratology*, *52*(Pt B), 194–209. https://doi.org/10.1016/j.ntt.2015.08.010

Karnaky, K. J. (1986). Structure and Function of the Chloride Cell of Fundulus heteroclitus and Other Teleosts. *Integrative and Comparative Biology*, *26*(1), 209–224. https://doi.org/10.1093/ICB/26.1.209

Kennard, A. S., & Theriot, J. A. (2020). Osmolarity-independent electrical cues guide rapid response to injury in zebrafish epidermis. *ELife*, *9*, 1–27. https://doi.org/10.7554/ELIFE.62386

Kiener, T. K., Selptsova-Friedrich, I., & Hunziker, W. (2008). Tjp3/zo-3 is critical for epidermal barrier function in zebrafish embryos. *Developmental Biology*, *316*(1), 36–49. https://doi.org/10.1016/J.YDBIO.2007.12.047

Kim, J. W., Isobe, T., Chang, K. H., Amano, A., Maneja, R. H., Zamora, P. B., Siringan, F. P., & Tanabe, S. (2011). Levels and distribution of organophosphorus flame retardants and plasticizers in fishes from Manila Bay, the Philippines. *Environmental Pollution*, *159*(12), 3653–3659. https://doi.org/10.1016/j.envpol.2011.07.020

Kim, S., Jung, J., Lee, I., Jung, D., Youn, H., & Choi, K. (2015). Thyroid disruption by triphenyl phosphate, an organophosphate flame retardant, in zebrafish (Danio rerio) embryos/larvae, and in GH3 and FRTL-5 cell lines. *Aquatic Toxicology*, *160*, 188–196. https://doi.org/10.1016/j.aquatox.2015.01.016

Klose, J., Pahl, M., Bartmann, K., Bendt, F., Blum, J., Dolde, X., Förster, N., Holzer, A. K., Hübenthal, U., Keßel, H. E., Koch, K., Masjosthusmann, S., Schneider, S., Stürzl, L. C., Woeste, S., Rossi, A., Covaci, A., Behl, M., Leist, M., … Fritsche, E. (2021). Neurodevelopmental toxicity assessment of flame retardants using a human DNT in vitro testing battery. *Cell Biology and Toxicology*, 1–27. https://doi.org/10.1007/s10565-021-09603-2

Kumai, Y., & Perry, S. F. (2012). Mechanisms and regulation of Na+ uptake by freshwater fish. *Respiratory Physiology & Neurobiology*, *184*(3), 249–256. https://doi.org/10.1016/J.RESP.2012.06.009

Kwong, R. W. M., Kumai, Y., & Perry, S. F. (2013). The Role of Aquaporin and Tight Junction Proteins in the Regulation of Water Movement in Larval Zebrafish (Danio rerio). *PLoS ONE*, *8*(8), e70764. https://doi.org/10.1371/journal.pone.0070764

Kwong, R. W. M., Kumai, Y., & Perry, S. F. (2014). The physiology of fish at low pH: the zebrafish as a model system. *Journal of Experimental Biology*, *217*(5), 651–662. https://doi.org/10.1242/JEB.091603

Kwong, R. W. M., Kumai, Y., & Perry, S. F. (2016). Neuroendocrine control of ionic balance in zebrafish. *General and Comparative Endocrinology*, *234*, 40–46. https://doi.org/10.1016/J.YGCEN.2016.05.016

Kwong, R. W. M., & Perry, S. F. (2013). The tight junction protein claudin-b regulates epithelial permeability and sodium handling in larval zebrafish, Danio rerio. *American Journal of Physiology - Regulatory, Integrative and Comparative Physiology*, *304*(7), R504. https://doi.org/10.1152/AJPREGU.00385.2012

Kwong, R. W. M., & Perry, S. F. (2015). An essential role for parathyroid hormone in gill formation and differentiation of ion-transporting cells in developing zebrafish. *Endocrinology*, *156*(7), 2384–2394. https://doi.org/10.1210/en.2014-1968

Laurent, P. (1984). 2 Gill Internal Morphology. *Fish Physiology*, *10*(PA), 73–183. https://doi.org/10.1016/S1546-5098(08)60318-0

Le Guellec, D., Morvan-Dubois, G., & Sire, J. Y. (2003). Skin development in bony fish with particular emphasis on collagen deposition in the dermis of the zebrafish (Danio rerio). *International Journal of Developmental Biology*, *48*(2–3), 217–231. https://doi.org/10.1387/IJDB.15272388

LeBert, D. C., & Huttenlocher, A. (2014). Inflammation and wound repair. In *Seminars in Immunology* (Vol. 26, Issue 4, pp. 315–320). https://doi.org/10.1016/j.smim.2014.04.007

Leguen, I., Le Cam, A., Montfort, J., Peron, S., & Fautrel, A. (2015). Transcriptomic analysis of trout gill ionocytes in fresh water and sea water using laser capture microdissection combined with microarray analysis. *PLoS ONE*, *10*(10). https://doi.org/10.1371/journal.pone.0139938

Li, J., Xie, Z., Mi, W., Lai, S., Tian, C., Emeis, K.-C., & Ebinghaus, R. (2017). Organophosphate Esters in Air, Snow, and Seawater in the North Atlantic and the Arctic. *Environmental Science and Technology*, *51*(12), 6887–6896. https://doi.org/10.1021/ACS.EST.7B01289

Li, Q., Frank, M., Thisse, C. I., Thisse, B. V., & Uitto, J. (2011). Zebrafish: A Model System to Study Heritable Skin Diseases. *Journal of Investigative Dermatology*, *131*(3), 565–571. https://doi.org/10.1038/JID.2010.388

Li, X., Gao, A., Wang, Y., Chen, M., Peng, J., Yan, H., Zhao, X., Feng, X., & Chen, D. (2016). Alcohol exposure leads to unrecoverable cardiovascular defects along with edema and motor function changes in developing zebrafish larvae. *Biology Open*, *5*(8), 1128. https://doi.org/10.1242/BIO.019497

Li, Y., Wang, C., Zhao, F., Zhang, S., Chen, R., & Hu, J. (2018). Environmentally Relevant Concentrations of the Organophosphorus Flame Retardant Triphenyl Phosphate Impaired Testicular Development and Reproductive Behaviors in Japanese Medaka (Oryzias latipes). *Environmental Science & Technology*, *5*(11), 649–654. https://doi.org/10.1021/acs.estlett.8b00546

Lin, C. H., Hu, H. J., & Hwang, P. P. (2016). Cortisol regulates sodium homeostasis by stimulating the transcription of sodium-chloride transporter (NCC) in zebrafish (Danio rerio). *Molecular and Cellular Endocrinology*, *422*, 93–102. https://doi.org/10.1016/J.MCE.2015.12.001

Lin, C. H., Huang, C. L., Yang, C. H., Lee, T. H., & Hwang, P. P. (2004). Time-course changes in the expression of Na, K-ATPase and the morphometry of mitochondrion-rich cells in gills of euryhaline tilapia (Oreochromis mossambicus) during freshwater acclimation. *Journal of Experimental Zoology. Part A, Comparative Experimental Biology*, *301*(1), 85–96. https://doi.org/10.1002/JEZ.A.20007

Link, V., Shevchenko, A., & Heisenberg, C. P. (2006). Proteomics of early zebrafish embryos. *BMC Developmental Biology*, *6*. https://doi.org/10.1186/1471-213X-6-1

Liu, S. T., Chou, M. Y., Wu, L. C., Horng, J. L., & Lin, L. Y. (2020). Transient receptor potential vanilloid 4 modulates ion balance through the isotocin pathway in zebrafish (Danio rerio). *American Journal of Physiology. Regulatory, Integrative and Comparative Physiology*. https://doi.org/10.1152/ajpregu.00307.2019

Liu, X., Ji, K., & Choi, K. (2012). Endocrine disruption potentials of organophosphate flame retardants and related mechanisms in H295R and MVLN cell lines and in zebrafish. *Aquatic Toxicology*, *114–115*, 173–181. https://doi.org/10.1016/J.AQUATOX.2012.02.019

Liu, X., Jung, D., Jo, A., Ji, K., Moon, H.-B. B., & Choi, K. (2016). Long-term exposure to triphenylphosphate alters hormone balance and HPG, HPI, and HPT gene expression in zebrafish (Danio rerio). *Environmental Toxicology and Chemistry*, *35*(9), 2288–2296. https://doi.org/10.1002/etc.3395

Manzon, L. A. (2002). The Role of Prolactin in Manzon, L. A. (2002). The Role of Prolactin in Fish Osmoregulation: A Review. General and Comparative Endocrinology, 125(2), 291–310. https://doi.org/10.1006/GCEN.2001.7746Fish Osmoregulation: A Review. *General and Comparative Endocrinology*, *125*(2), 291–310. https://doi.org/10.1006/GCEN.2001.7746

Marshall, W. S., Bryson, S. E., Darling, P., Whitten, C., Patrick, M., Wilkie, M., Wood, C. M., & Buckland-Nicks, J. (1997). NaCl transport and ultrastructure of opercular epithelium from a freshwater-adapted euryhaline teleost,Fundulus heteroclitus. *The Journal of Experimental Zoology*, *277*(1), 23–37. https://doi.org/10.1002/(SICI)1097-010X(19970101)277:1<23::AID-JEZ3>3.0.CO;2-D

Matsukami, H., Suzuki, G., Tue, N. M., Tuyen, L. H., Viet, P. H., Takahashi, S., Tanabe, S., & Takigami, H. (2016). Analysis of monomeric and oligomeric organophosphorus flame retardants in fish muscle tissues using liquid chromatography–electrospray ionization tandem mass spectrometry: Application to Nile tilapia (Oreochromis niloticus) from an e-waste processing area. *Emerging Contaminants*, *2*(2), 89–97. https://doi.org/10.1016/j.emcon.2016.03.004

McCollum, C. W., Conde-Vancells, J., Hans, C., Vazquez-Chantada, M., Kleinstreuer, N., Tal, T., Knudsen, T., Shah, S. S., Merchant, F. A., Finnell, R. H., Gustafsson, J. Å., Cabrera, R., & Bondesson, M. (2017). Identification of vascular disruptor compounds by analysis in zebrafish embryos and mouse embryonic endothelial cells. *Reproductive Toxicology*, *70*, 60–69. https://doi.org/10.1016/J.REPROTOX.2016.11.005

Mccollum, C. W., Ducharme, N. A., Bondesson, M., & Gustafsson, J. A. (2011). Developmental toxicity screening in zebrafish. *Birth Defects Research Part C: Embryo Today: Reviews*, *93*(2), 67–114. https://doi.org/10.1002/BDRC.20210

McCormick, S. D., & Bradshaw, D. (2006). Hormonal control of salt and water balance in vertebrates. *General and Comparative Endocrinology*, *147*(1), 3–8. https://doi.org/10.1016/J.YGCEN.2005.12.009

McGee, S. P., Konstantinov, A., Stapleton, H. M., & Volz, D. C. (2013). Aryl phosphate esters within a major pentaBDE replacement product induce cardiotoxicity in developing zebrafish embryos: Potential role of the aryl hydrocarbon receptor. *Toxicological Sciences*, *133*(1), 144–156. https://doi.org/10.1093/toxsci/kft020

McGruer, V., Tanabe, P., Vliet, S. M. F., Dasgupta, S., Qian, L., Volz, D. C., & Schlenk, D. (2021). Effects of Phenanthrene Exposure on Cholesterol Homeostasis and Cardiotoxicity in Zebrafish Embryos. *Environmental Toxicology and Chemistry*, *40*(6), 1586–1595. https://doi.org/10.1002/ETC.5002

Mitchell, C. A., Dasgupta, S., Zhang, S., Stapleton, H. M., & Volz, D. C. (2018). Disruption of nuclear receptor signaling alters triphenyl phosphate-induced cardiotoxicity in zebrafish embryos. *Toxicological Sciences*, *163*(1), 307–318. https://doi.org/10.1093/toxsci/kfy037

Mitchell, C. A., Reddam, A., Dasgupta, S., Zhang, S., Stapleton, H. M., & Volz, D. C. (2019). Diphenyl Phosphate-Induced Toxicity during Embryonic Development. *Environmental Science and Technology*, *53*(7), 3908–3916. https://doi.org/10.1021/acs.est.8b07238

Naomi, R., Bahari, H., Yazid, M. D., Embong, H., & Othman, F. (2021). Zebrafish as a Model System to Study the Mechanism of Cutaneous Wound Healing and Drug Discovery: Advantages and Challenges. *Pharmaceuticals*, *14*(10), 1058. https://doi.org/10.3390/PH14101058

Narumanchi, S., Wang, H., Perttunen, S., Tikkanen, I., Lakkisto, P., & Paavola, J. (2021). Zebrafish Heart Failure Models. *Frontiers in Cell and Developmental Biology*, *9*, 1061. https://doi.org/10.3389/FCELL.2021.662583/XML/NLM

Nesan, D., & Vijayan, M. M. (2012). Embryo exposure to elevated cortisol level leads to cardiac performance dysfunction in zebrafish. *Molecular and Cellular Endocrinology*, *363*(1–2), 85–91. https://doi.org/10.1016/J.MCE.2012.07.010

Oliveira, R., Domingues, I., Grisolia, C. K., & Soares, A. M. V. M. (2009). Effects of triclosan on zebrafish early-life stages and adults. *Environmental Science and Pollution Research International*, *16*(6), 679–688. https://doi.org/10.1007/S11356-009-0119-3

Oliveri, A. N., Bailey, J. M., & Levin, E. D. (2015). Developmental exposure to organophosphate flame retardants causes behavioral effects in larval and adult zebrafish. *Neurotoxicology and Teratology*, *52*(Pt B), 220–227. https://doi.org/10.1016/j.ntt.2015.08.008

Papich, M. G. (2016). Mannitol. *Saunders Handbook of Veterinary Drugs*, 470–471. https://doi.org/10.1016/B978-0-323-24485-5.00352-1

Pelster, B., & Burggren, W. W. (1996). Disruption of hemoglobin oxygen transport does not impact oxygen-dependent physiological processes in developing embryos of zebra fish (Danio rerio). *Circulation Research*, *79*(2), 358–362. https://doi.org/10.1161/01.RES.79.2.358

Peng, G., He, Y., Zhao, M., Yu, T., Qin, Y., & Lin, S. (2018). Differential effects of metal oxide nanoparticles on zebrafish embryos and developing larvae. *Environmental Science: Nano*, *5*(5), 1200–1207. https://doi.org/10.1039/C8EN00190A

Pikula, J., Pojezdal, L., Papezikova, I., Minarova, H., Mikulikova, I., Bandouchova, H., Blahova, J., Bednarska, M., Mares, J., & Palikova, M. (2021). Carp Edema Virus Infection Is Associated With Severe Metabolic Disturbance in Fish. *Frontiers in Veterinary Science*, *8*, 505. https://doi.org/10.3389/FVETS.2021.679970/BIBTEX

Pinheiro-da-Silva, J., & Luchiari, A. C. (2021). Embryonic ethanol exposure on zebrafish early development. *Brain and Behavior*, *11*(6), e02062. https://doi.org/10.1002/BRB3.2062

Pott, A., Bock, S., Berger, I. M., Frese, K., Dahme, T., Keßler, M., Rinné, S., Decher, N., Just, S., & Rottbauer, W. (2018). Mutation of the Na+/K+-ATPase Atp1a1a.1 causes QT interval prolongation and bradycardia in zebrafish. *Journal of Molecular and Cellular Cardiology*, *120*, 42–52. https://doi.org/10.1016/j.yjmcc.2018.05.005

Ramesh, M., Angitha, S., Haritha, S., Poopal, R. K., Ren, Z., & Umamaheswari, S. (2020). Organophosphorus flame retardant induced hepatotoxicity and brain AChE inhibition on zebrafish (Danio rerio). *Neurotoxicology and Teratology*, *82*, 106919. https://doi.org/10.1016/j.ntt.2020.106919

Reddam, A., Mitchell, C. A., Dasgupta, S., Kirkwood, J. S., Vollaro, A., Hur, M., & Volz, D. C. (2019). mRNA-Sequencing Identifies Liver as a Potential Target Organ for Triphenyl Phosphate in Embryonic Zebrafish. *Toxicological Sciences*. https://doi.org/10.1093/toxsci/kfz169

Reemtsma, T., García-López, M., Rodríguez, I., Quintana, J. B., & Rodil, R. (2008). Organophosphorus flame retardants and plasticizers in water and air I. Occurrence and fate. *TrAC - Trends in Analytical Chemistry*, *27*(9), 727–737. https://doi.org/10.1016/j.trac.2008.07.002

Richardson, R. J. (2018). Parallels between vertebrate cardiac and cutaneous wound healing and regeneration. *Npj Regenerative Medicine*, *3*, 21. https://doi.org/10.1038/s41536-018-0059-y

Rombough, P. (2007). The functional ontogeny of the teleost gill: Which comes first, gas or ion exchange? *Comparative Biochemistry and Physiology Part A: Molecular & Integrative Physiology*, *148*(4), 732–742. https://doi.org/10.1016/j.cbpa.2007.03.007

Rosowski, E. E. (2020). Determining macrophage versus neutrophil contributions to innate immunity using larval zebrafish. *DMM Disease Models and Mechanisms*, *13*(1). https://doi.org/10.1242/DMM.041889/223112

Sant, K. E., & Timme-Laragy, A. R. (2018). *Zebrafish as a Model for Toxicological Perturbation of Yolk and Nutrition in the Early Embryo*. *5*(1). /pmc/articles/PMC5876134/

Serluca, F. C., Drummond, I. A., & Fishman, M. C. (2002). Endothelial signaling in kidney morphogenesis: A role for hemodynamic forces. *Current Biology*, *12*(6), 492–497. https://doi.org/10.1016/S0960-9822(02)00694-2/ATTACHMENT/5BA67E49-4807-453E-8B8B-087457139F67/MMC1.PDF

Shi, Q., Wang, M., Shi, F., Yang, L., Guo, Y., Feng, C., Liu, J., & Zhou, B. (2018). Developmental neurotoxicity of triphenyl phosphate in zebrafish larvae. *Aquatic Toxicology*, *203*, 80–87. https://doi.org/10.1016/j.aquatox.2018.08.001

Shi, Q., Wang, Z., Chen, L., Fu, J., Han, J., Hu, B., & Zhou, B. (2019). Optical toxicity of triphenyl phosphate in zebrafish larvae. *Aquatic Toxicology*, *210*, 139–147. https://doi.org/10.1016/j.aquatox.2019.02.024

Shu, X., Cheng, K., Patel, N., Chen, F., Joseph, E., Tsai, H. J., & Chen, J. N. (2003). Na,K-ATPase is essential for embryonic heart development in the zebrafish. *Development*, *130*(25), 6165–6173. https://doi.org/10.1242/dev.00844

Shu, Y., Lou, Q., Dai, Z., Dai, X., He, J., Hu, W., & Yin, Z. (2016). The basal function of teleost prolactin as a key regulator on ion uptake identified with zebrafish knockout models. *Scientific Reports 2016 6:1*, *6*(1), 1–12. https://doi.org/10.1038/srep18597

Song, Q., Feng, Y., Liu, G., & Lv, W. (2019). Degradation of the flame retardant triphenyl phosphate by ferrous ion-activated hydrogen peroxide and persulfate: Kinetics, pathways, and mechanisms. *Chemical Engineering Journal*, *361*, 929–936. https://doi.org/10.1016/j.cej.2018.12.140

Souder, J. P., & Gorelick, D. A. (2017). Quantification of Estradiol Uptake in Zebrafish Embryos and Larvae. *Toxicological Sciences : An Official Journal of the Society of Toxicology*, *158*(2), 465–474. https://doi.org/10.1093/TOXSCI/KFX107

Stainier, D. Y. R., & Fishman, M. C. (1992). Patterning the zebrafish heart tube: Acquisition of anteroposterior polarity. *Developmental Biology*, *153*(1), 91–101. https://doi.org/10.1016/0012-1606(92)90094-W

Stapleton, H. M., Klosterhaus, S., Eagle, S., Fuh, J., Meeker, J. D., Blum, A., & Webster, T. F. (2009). Detection of organophosphate flame retardants in furniture foam and U.S. house dust. *Environmental Science and Technology*, *43*(19), 7490–7495. https://doi.org/10.1021/es9014019

Szymański, Ł., Skopek, R., Palusińska, M., Schenk, T., Stengel, S., Lewicki, S., Kraj, L., Kamiński, P., & Zelent, A. (2020). Retinoic Acid and Its Derivatives in Skin. *Cells*, *9*(12), 1–14. https://doi.org/10.3390/cells9122660

Takada, M., & Kasai, M. (2003). Prolactin increases open-channel density of epithelial Na+ channel in adult frog skin. *The Journal of Experimental Biology*, *206*(Pt 8), 1319–1323. https://doi.org/10.1242/JEB.00266

Takei, Y., Hiroi, J., Takahashi, H., & Sakamoto, T. (2014). Diverse mechanisms for body fluid regulation in teleost fishes. *American Journal of Physiology. Regulatory, Integrative and Comparative Physiology*, *307*(7), R778–R792. https://doi.org/10.1152/AJPREGU.00104.2014

Thakur, P. C., Davison, J. M., Stuckenholz, C., Lu, L., & Bahary, N. (2014). Dysregulated phosphatidylinositol signaling promotes endoplasmic-reticulum- stress-mediated intestinal mucosal injury and inflammation in zebrafish. *DMM Disease Models and Mechanisms*, *7*(1), 93–106. https://doi.org/10.1242/DMM.012864/258750/AM/DYSREGULATED-PHOSPHATIDYLINOSITOL-SIGNALING

Tingaud-Sequeira, A., Calusinska, M., Finn, R. N., Chauvigné, F., Lozano, J., & Cerdà, J. (2010). The zebrafish genome encodes the largest vertebrate repertoire of functional aquaporins with dual paralogy and substrate specificities similar to mammals. *BMC Evolutionary Biology*, *10*(1), 1–18. https://doi.org/10.1186/1471-2148-10-38/FIGURES/8

Turksen, K., & Troy, T. C. (2004). Barriers built on claudins. *Journal of Cell Science*, *117*(12), 2435–2447. https://doi.org/10.1242/JCS.01235

van der Veen, I., & de Boer, J. (2012). Phosphorus flame retardants: Properties, production, environmental occurrence, toxicity and analysis. In *Chemosphere* (Vol. 88, Issue 10, pp. 1119–1153). Pergamon. https://doi.org/10.1016/j.chemosphere.2012.03.067

Wiegand, J., Avila-Barnard, S., Nemarugommula, C., Lyons, D., Zhang, S., Stapleton, H. M., & Volz, D. C. (2023). Triphenyl phosphate-induced pericardial edema in zebrafish embryos is dependent on the ionic strength of exposure media. *Environment International*, *173*, 107757. https://doi.org/10.1016/J.ENVINT.2023.107757

Wiegand, J., Cheng, V., Reddam, A., Avila-Barnard, S., & Volz, D. C. (2022). Triphenyl phosphate-induced pericardial edema is associated with elevated epidermal ionocytes within zebrafish embryos. *Environmental Toxicology and Pharmacology*, *89*, 103776. https://doi.org/10.1016/j.etap.2021.103776

Wilson, J. M., & Laurent, P. (2002). Fish gill morphology: inside out. *The Journal of Experimental Zoology*, *293*(3), 192–213. https://doi.org/10.1002/JEZ.10124

Wright, P. A., & Wood, C. M. (2012). Seven things fish know about ammonia and we don't. *Respiratory Physiology & Neurobiology*, *184*(3), 231–240. https://doi.org/10.1016/J.RESP.2012.07.003

Xie, Y., Meijer, A. H., & Schaaf, M. J. M. (2021). Modeling Inflammation in Zebrafish for the Development of Anti-inflammatory Drugs. *Frontiers in Cell and Developmental Biology*, *0*, 1819. https://doi.org/10.3389/FCELL.2020.620984

Yan, J. J., & Hwang, P. P. (2019). Novel discoveries in acid-base regulation and osmoregulation: A review of selected hormonal actions in zebrafish and medaka. *General and Comparative Endocrinology*, *277*, 20–29. https://doi.org/10.1016/J.YGCEN.2019.03.007

Yang, J., Zhao, Y., Li, M., Du, M., Li, X., & Li, Y. (2019). A review of a class of emerging contaminants: The classification, distribution, intensity of consumption, synthesis routes, environmental effects and expectation of pollution abatement to organophosphate flame retardants (opfrs). In *International Journal of Molecular Sciences* (Vol. 20, Issue 12). MDPI AG. https://doi.org/10.3390/ijms20122874

Yozzo, K., Isales, G., Rafferty, & Volz, D. (2013). High-content screening assay for identification of chemicals impacting cardiovascular function in zebrafish embryos. *Environmental Science & Technology*, *47*(19), 11302–11310. https://doi.org/10.1021/ES403360Y

Yozzo, K. L., McGee, S. P., & Volz, D. C. (2013). Adverse outcome pathways during zebrafish embryogenesis: A case study with paraoxon. *Aquatic Toxicology*, *126*, 346–354. https://doi.org/10.1016/J.AQUATOX.2012.09.008